Autonomous regulation of mast cell degranulation through an inhibitory receptor CD300a

（抑制性受容体 CD300a を介した
肥満細胞脱顆粒の自己調節）

2019

筑波大学グローバル教育院
School of Integrative and Global Majors,
University of Tsukuba
Ph.D. Program in Human Biology

Yaqiu Wang

Table of Contents

0. Abstract

Although phosphatidylserine (PS) confined to the inner leaflets of plasma membrane is exposed on the cell surface when cells undergo apoptosis, viable cells also externalize PS in certain cellular states. However, the pathophysiological significance of PS exposure on viable cells remains elusive. Through imaging analyses, we found that PS was exposed on the plasma membrane of live mast cells (MCs) during degranulation. Although the exposed PS did not promote phagocytes engulfment of live MCs, it colocalized with CD300a, an inhibitory immunoreceptor that recognizes PS. Fluorescence resonance energy transfer (FRET) experiment reveals the direct *cis*-binding between CD300a and PS during degranulation. Functionally, I observed that degranulation was greater after stimulation with an IgE–antigen complex in MCs deficient in CD300a than in wild-type MCs. Pretreatment of MCs with a neutralizing anti-CD300a antibody efficiently upregulated the degranulation of wild-type MCs as a result of interference of *cis*-interaction between CD300a and PS as evidenced by decreased FRET efficiency. Consistently, CD300a-deficient mice or in vivo treatment with a neutralizing CD300a antibody showed slower recovery of body temperature compared with wild-type mice in MCs-dependent passive systemic anaphylaxis. Our study suggests self-regulation of MC degranulation through *cis*-interaction of PS with CD300a to down regulate allergic response, adding another layer of regulation in allergic responses.

Keywords: Phosphatidylserine; mast cell degranulation; CD300a; self-regulation

1. Introduction

1.1 Mast cells and allergic response

Mast cells (MCs) are one of the evolutionally conserved cell types among all the vertebrate[1]. First described by German physician Paul Ehrlich in 1878 based on its unique cellular morphology with granules and the ability to retain basic aniline dyes, MCs are widely distributed among many tissues, including vital organs such as brain, intestine, skin and lungs. The heterogenicity of MCs is now a well-established concept, as two distinct MCs populations – mucosal-type MCs and connective tissue-type MCs – could be defined in rodents based on their different expression profile of MCs protease[2]; and three different populations of human MCs are proposed by their different serine proteases expression, namely, tryptase-only (MC_T), chymase-only (MC_C), and tryptase and chymase double positive (MC_{TC}) MCs[3].

It is now appreciated for MCs' important roles in mammalian physiology and pathology[4]. Despite the increasing research interests of MCs roles in normal physiology, such as angiogenesis, tissue remodeling, wound healing and immune regulation, the effector function of MCs activation in allergic response remain to be a significant research area[5] .

Although MCs are the major effector cell type involved in IgE-dependent allergic responses, the link between MCs activation and allergic symptoms (e.g. anaphylactic shock) was only established half century later after the discovery of MCs, when histamine and heparin, the major effector molecules for anaphylactic shock, were found mainly released from MCs by series works from Riley and West in 1950s[6–8]. In 1966 and 1967, K Ishizaka and T Ishizaka found IgE and their reactivity to specific allergen were correlated and responsible, respectively, of the

hypersensitivity-induction activity from atopic patients[9,10]. The successful culture of rat basophilic leukemia cell line (RBL) later on enabled the detailed characterization of IgE-binding property of basophil and mast cell, as well as the histamine release from some RBL cells after IgE binding[11,12] . Finally, in 1989, the complete structure of high affinity IgE receptor FcεRI was cloned and expressed[13].

It is clear now that antigen-specific IgE sensitize MCs through binding to the IgE binding site on α chain of FcεRI. The presence of multivalent antigen aggregates more than one FcεRI. The colligation of this receptor activates MCs and cause the release of pro-allergic substances, a process termed "degranulation", as the granules which contain the pre-stored pro-allergic substances, are released during such MC activation. Besides histamine and heparin, the activation of MCs also triggers the release of a large panel of other effector molecules, including cytokines, such as TNF-α[13] and various proteases[13]. Activated MCs are also capable of releasing lipid mediators, chemokines and growth factors through *de novo* synthesis[14,15]. The released mediators play important roles in not only allergic responses, but also bacteria killing[16,17], leukocyte recruitment [18,19] and adaptive immune response induction[20].

The importance of MCs in physiology and pathology is revealed using MC-deficient mice as powerful research tools[21–23]. Indeed, MC-deficient mice are completely protected from IgE-mediated passive systemic anaphylactic shock, highlighting the vital role of MCs as effector cells during anaphylactic shock[24]. Reconstituting MCs in MC-deficient mice is a compelling method to dissect the critical pathways and regulatory components involved in MC degranulation, allergy and anaphylaxis. CD300lf and Allergin-1, for example, are inhibitory receptors on MCs and inhibit FcεRI-mediated degranulation. Transfer of CD300lf[24] or Allergin-1[25] deficient MCs into MC-deficient mice showed more body temperature decrease

than wild-type MCs-transferred group in a passive systemic anaphylaxis (PSA) model, confirming the inhibitory function of these receptors *in vivo*. Using such strategy, studies identified many factors regulating mast cell degranulation and their further implications in allergy and anaphylaxis[26–28].

1.2 Mast cell degranulation machinery and its regulation by inhibitory receptors

On MCs, FcεRI is composed of one each of α and β chain with two γ chains. β and γ chains contain immunoreceptor tyrosine-based activation motifs (ITAMs). Upon colligation, ITAMs in both β and γ chains are quickly phosphorylated by the Src family kinase Lyn, which is constantly associated with β chain. The phosphorylation of ITAMs results in the Syk recruitment to the γ chain and Syk phosphorylation. Phosphorylated Syk further phosphorylate other adaptor proteins and kinases in the signal cascade, including phospholipase C gamma (PLC γ), a key molecule to catalyze the hydrolysis of phosphatidylinositol bisphosphate to inositol trisphosphate (IP3) and diacylglycerol (DAG), which result in cytosolic Ca^{2+} mobilization and protein kinase C (PKC) activation, respectively. The activated PKC further phosphorylate the light chain of myosin within the actin-myosin complex under cytoplasm membrane and cause the disassembly of the complex. SNARE complex is formed as a result of increased cytosolic calcium and the inactivation of its inhibitory machineries by activated PKC. Formed SNARE complexes mediate the membrane fusion between granules and cytoplasmic membrane, which results in the release of processed granule contents as well as the change of surface markers of the cytoplasmic protein (Fig. 1).[29]

The consequences after granules and cytoplasm membrane fusion provide sensitive and complementary methods for measuring the degranulation

experimentally. For example, the release of histamine[30], serotonin[31] , catalytic enzymes (e.g. beta-hexosaminidase)[32] and cell surface expression of endosomal markers (e.g. LAMP-1)[33] are frequently used for such propose.

The degranulation process is a well-organized cellular and molecular event with the cooperation among various pathways and signaling molecules aforementioned. The defects of certain components involved in this event will cause the altered degranulation and subsequent change of *in vivo* phenotype (e.g. allergic response, anaphylaxis)[33] . For example, the genetic deletion of FcεRI α chain causes a complete loss of degranulation of MCs and therefore the MCs-deficient mice receiving a transfer of FcεRI α-deficient MCs are protected from allergic symptoms in a food allergy model[27].

The deficiency of src-famlimy kinase Lyn, however, generates confusing results with decreased[34,35], increased[35,36] and comparable[37] degranulation in vitro, as well as controversial phenotypes *in vivo*. This is probably because of the multiple functions of Lyn to process inhibitory phosphorylation on C-terminal Src kinase (Csk)-binding protein (Cbp)[36] and on the FcεRI β chain[35] , as well as the increased activation of SHIP-1 phosphatase activity in Lyn-deficient MCs[38].

The Syk-deficient MCs showed defect to phosphorylate both PLCγ1 and PLCγ2 and failed to increase the cytosolic calcium concentration upon FcεRI activation and failed to degranulate[39]. Similarly, PLCγ2 deficient MCs showed impaired calcium mobilization, therefore a decreased degranulation in response to FcεRI stimulation[40].

The pathology of allergic diseases and anaphylaxis is largely contributed by mast cell degranulation triggered by FcεRI activation[24,41]. Therefore, the specific inhibitory machinery of degranulation is thought to be of therapeutic significance[42,43]. Indeed, many approaches showed promising results in inhibiting the

MCs degranulation, including using the inhibitors of key signaling pathways[44,45], modulation of actin-regulatory proteins[46] and cell intrinsic SNARE inhibitory proteins[47] as well as ITIM-bearing cell surface receptors[42,48].

Because the molecules involved in degranulation signal transduction and machinery are often found to be universally expressed in other cell types and have fundamental functions in steady state (e.g. SNARE[49] proteins and actin[50]), which rendered their specificity for targeting MCs degranulation. On the other hand, MCs naturally express many inhibitory receptors which bearing the immunoreceptor tyrosine-based inhibition motif (ITIM) in their cytoplasmic domains (e.g. FcRIIB[51], gp49B1[52], SIRPα[53], LILRB2[54], CD300a[55], CD300lf[56] and Allergin-1[25]). These receptors are expressed on more specific cell populations and specifically be activated in the presence of their ligands or agonistic antibodies[42]. Upon activation, phosphorylation of tyrosine residues in ITIMs enables the recruiting of phosphatase such as SHP-1, SHP-2 and/or SHIP, which will dephosphorylate several kinases and their downstream targets of the FcεRI pathway, thus suppresses MC activation. For example, colligation of FcεRI with ITIM bearing receptors, such as gp49B1[52], CD300lf[57] and Allergin-1[25] with receptor-specific monoclonal antibodies, showed effective decrease of FcεRI-mediated mast cell degranulation without obvious requirement of their natural ligands.

Among the inhibitory receptors on MCs, LILRB2 is able to suppress FcεRI-mediated mast cell degranulation without colligation with FcεRI. Indeed, the ligand of LILRB2 is found to be MHC-I, which is originally expressed on the same cell and form constant cis-interaction and activation of LILRB2. Such cis-interaction may regulate the activation threshold of MCs[54] .

In contrast, CD300lf shows intriguing requirement of its proposed ligands for inhibitory function. Izawa and colleagues identified ceramide as natural ligands of

mouse CD300lf and blocking interaction of ceramide and CD300lf by an anti-ceramide antibody effectively abolished the inhibitory function of CD300lf in a passive cutaneous anaphylaxis model, resulting in elevated vascular leakage[57]. Indicating the inhibitory function of indigenous ceramide through its receptor CD300lf, intriguingly however, exogenous administration of ceramide could also negatively regulate MCs function in the same model in a CD300lf dependent manner[57], raising a question of the relative importance of indigenous ceramide in CD300lf function.

Although therapeutically effective, in many cases, the physiological significance of those inhibitory receptors on MCs remains unknown due to lack of knowledge of their natural ligands[42,48], proposing a big challenge for therapeutically targeting. (Fig. 1)

1.3 PS exposure during apoptosis and cell activation

Eukaryotic cell membrane is composited of lipids, proteins and carbohydrates, with the lipid bilayers as scaffold, membrane proteins stay in or anchored on the lipid bilayer and carbohydrates mainly exist as glycolipid or glycoprotein[58]. The lipid compartment is mainly consisted of phospholipids, sphingolipids and sterols[59]. Although the exact composition of lipids differs across cell types and status, the major structural lipids in eukaryotic membrane is phospholipids: phosphatidylcholine (PC), phosphatidylethanolamine (PE), phosphatidylserine (PS), phosphatidylinositol (PI) and phosphatidic acid (PA), with PC as dominant component (>50%) [59,60]. One important feature of the lipid bilayer is the asymmetric distribution of lipid components on live cells, with consists predominantly of PC, sphingomyelin, and glycolipids dominant the outer leaflet, whereas the inner leaflet

contains PE, PS and PI and cholesterol is distributed in both leaflets[58]. The asymmetric distribution is largely due to the P4-ATPases flippase activity, which translocate the aminophospholipids PS and PE towards the cytosolic leaflet[61,62]. However, PS is exposed on the surface after death induction (e.g. apoptosis) or cell activation[63–66].

During cell apoptosis, PS exposure can be triggered by the inactivation of flippase as well as the activation of scramblase, a group of enzymes functioning to transport lipids following the existing lipid gradient without specificity and direction between the inner and outer leaflets[67,68]. Nagata's group identified a caspase cleavage site in a flippase ATP11C and a scramblase Xkr8. The activation of caspase during apoptosis causes the cleavage and inactivation of ATP11C together with cleavage and activation of Xkr8 and lead to the exposure of PS during apoptosis; indeed, a mutation on the caspase cleavage site maintained the ATP11C flippase activity or suppressed Xkr8 activation during apoptosis and results in lack of PS exposure and resistance to phagocytosis [69,70].

Upon cell activation, Elliott and colleagues found that PS can be exposed on CD45RB negative T cell population as well as T cell activated through P2X7 receptor by ATP[64]. Similarly, the same group also reported that B cell PS exposure is also negatively correlated with CD45 phosphatase activity, as CD45-deficient B cells expose PS constantly on their surface[63]. Interestingly, PS exposure on activated platelets is caused by the increased cytosolic calcium concentration, where a calcium-dependent scramblase TMEM16F is activated in high calcium environment. Lack of TMEM16F dampens the PS exposure during platelet activation[71]. Indeed, a constitutive active form of TMEM16F is enough to expose PS on the cell surface when transduced into lymphoma cell[72]. Although, the responsible flippase and/or

scramblase remain unknown in both PS^+ live T and B cells, PS exposure on activated T cell was also correlated with increased cytosolic calcium[64] , pointing out the possibility for a calcium-dependent scramblase during PS exposure of activating T cell.

1.4 The function of apoptotic PS exposure

PS exposed on apoptotic cell is well-known as an "eat me" signal which promotes its recognition and engulfment by macrophages[73,74]. Accordingly, macrophages express receptors recognizing PS (e.g. Tim-4) and bridging proteins binding to PS (e.g. ProteinS, Gas6) to mediate receptor tyrosine kinase Tyro3/Axl/Mer (TAM)-dependent phagocytosis[75]. PS exposure on apoptotic cells is an important factor contributing to phagocytosis, since incubating apoptotic cells with PS masking molecule, Annxin-V[76] or a mutated Milk fat globule-EGF-factor 8 (MFG-E8-D89E)[77] efficiently decreased the phagocytosis of apoptotic cells by macrophages. Nagata's group proposed a "two-step" engulfment model for apoptotic cell phagocytosis, tethering and engulfing. PS may participate in both steps, as in an artificial Baf3 phagocytes expressing PS receptor Tim4 and integrin α(v)β(3), Tim-4 function as tethering through PS binding and integrin α(v)β(3) complex together with MFG-E8 mediate engulfment[78,79]. However, a recent study reported that Tim-4 may not be required for all the phagocytosis events in some types of macrophage[80] as Mer can function in both tethering and engulfing steps[81].

Besides functioning as an "eat me" signal, PS exposed on apoptotic cells also functions as a ligand for the PS receptor CD300a, expressed on many myeloid cells including MCs and dendritic cells (DCs). Nakahashi-Oda and colleagues found that PS from apoptotic epithelial cells bind to the same PS receptor CD300a on CD11b+

intestinal DCs and effectively suppressed TLR-4-TRIF-mediated interferon-β (IFNβ) production, a cytokine involved in regulatory T cell abundance. In an *in vitro* co-culture system of DCs and apoptotic cells, masking PS by MFG-E8-D89E dramatically increased the IFNβ from DCs to the similar level as CD300a deficient DCs after fecal contents stimulation[82]. Apoptotic cells are known for their immune regulatory ability[83], this finding highlighted the immune modulatory ability of apoptotic PS and its sensing machinery, as represented by a PS receptor CD300a.

1.5 The function of live cell PS exposure

As an "eat me" signal, PS-coated beads or PS liposomes can be effectively phagocytosed by macrophages[84–86], paradoxically, PS-exposing live cells are not sufficient to trigger phagocytosis, as a constitutive active scramblase-expressing lymphoma cell line, which expose comparable level of PS with that on apoptotic cells failed to be engulfed by phagocytes both *in vivo* and *in vitro*[72]. On the other hand, a recent report from the same group observed a loss-of-function mutation in flippase ATP11C conferred the PS exposure on live pre-B cells and pre-B cell-specific engulfment by macrophages in a PS-dependent manner[87]. It seems the flippase inactivation or scramblase activation induced PS exposure on living cell may differ from each other in the stability of surface PS and result in the distinct outcome of phagocytosis[69,73].

Despite the intriguing role of live cell exposed PS in live cell engulfment, the functions of PS exposed on activated platelet and T cells were investigated by different groups.

PS on activated platelets provides interacting platform for factor Va and Xa, interacts with proteins in prothrombinase complex and promotes its assembly[65,88],

explaining previous observation that PS-containing vesicles can sufficiently induce activation of prothrombinase in an *in vitro* artificial system[89]. Platelet incapable of exposing PS after activation due to a lack of scramblase TMEM16F failed to induce coagulation and mice with TMEM16F deficiency suffered from mild bleeding[71].

On T cell activated by ATP, PS exposure was shown to correlate with CD62L shedding[64]. In the same study, blocking PS by Annexin-V, inhibited the T cell migration both *in vitro* and *in vivo*[64]. However, the responsible molecules directly involved in PS translocation and recognition are still unknown. Moreover, PS exposure and its function on B cell are still controversial[63,90,91].

1.6 CD300a on MCs and live MCs PS exposure

MC is known to be AnnexinV positive upon FcεRI co-ligation induced degranulation [66,92,93]. The PS exposure is not associated with cell death and is reversible within 24 hr after stimulation[66,93]. However, the detailed characteristic (e.g. time scale, intensity) and physiological functions of PS externalization on MC remain elusive[94].

Interestingly, MCs highly express PS receptors CD300a which has three ITIMs in its cytoplasmic region[55] and was shown to be a receptor of phosphatidylserine (PS), which is expressed on apoptotic cells[95]. Nakahashi-Oda and colleagues reported that PS from apoptotic cells can robustly suppress the TLR-4-MyD88-mediated pro-inflammatory signals on MCs through interaction with MC CD300a. This suppression reduced the proinflammatory cytokine production in MCs during a murine sepsis model, rendered bacteria clearance and led to increased mortality[19]. Blocking CD300a and apoptotic PS interaction by a blocking antibody against CD300a or PS masking molecule MFG-E8-D89E, abolished the inhibitory

function of CD300a[19]. This study highlights the importance of CD300a in sensing apoptotic cells and mediating the immunosuppressive function during severe inflammation where apoptotic cells are abundant, however, apoptotic cells are quickly removed by phagocytes and therefore absent in normal tissue[96], raising a curiosity of CD300a function on MCs activation during non-inflammatory condition.

Despite the suggestions by many researchers that CD300a may play an inhibitory role in MC degranulation through its intracellular ITIM motifs after colligation with FcεRI receptor [94,97], little is known about the physiological function of CD300a on FcεRI-mediated MCs degranulation, especially the interaction between CD300a and its natural ligand PS, which is exposed during the degranulation.

2. Purpose of this study

Characterization of PS exposure during FcεRI-mediated MCs degranulation; functional analysis of externalized PS during MCs activation from the view of PS receptor CD300a.

3. Materials and methods

3.1 Cells

Bone marrow (BM)-derived cultured MCs (BMMCs) were generated by culturing wild-type (WT) and *Cd300a*$^{-/-}$ mouse BM cells in the presence of 10 ng/ml stem cell factor (SCF) (455-MC/CF, R&D Systems) and 4 ng/ml IL-3 (403-ML, R&D Systems) as previously described[25]. Briefly, weekly passages were performed by seeding 2 × 10^6 cells in 10 ml medium. Cells were cultured for 5 to 8 weeks before use. *Cd300a*$^{-/-}$ mice were described previously [25]. Cultured human synovial MCs were prepared and maintained as previously reported [98]. All mice experiments were conducted in accordance with the guidelines of the animal ethics committee of the University of Tsukuba Animal Research Center. The human mast cell study was approved by the Ethics Committee of the Nihon University School of Medicine (RK-160112-2), and all the subjects provided written informed consent in accordance with the Helsinki Declaration of the World Medical Association.

3.2 Antibodies, other reagents, and flow cytometry

Anti-mouse CD107a (1D4B), anti-mouse c-Kit (2B8), anti-mouse IgE (RME-1), mouse IgG1 (MOPC-21), anti-human CD107a (H4A3), anti-Flag (L5) antibodies and FITC-Avidin were purchased from Biolegend. Human IgE Myeloma (401152) was purchased from CALBIOCHEM. Anti-human IgE (Dε2) (E124.2.8) was purchased from BECKMAN COULTER. Annexin V, Trinitrophenyl (TNP)-specific mouse IgE (C38-2) was purchased from BD Bioscience. Anti-Syk (#2712) and anti-pSyk (#2711) antibodies were purchased from Cell Signaling Technology. TNP–ovalbumin (OVA), MFG-E8-D89E, MFG-E8-EPT, neutralizing and non-neutralizing anti-mouse CD300a antibodies (EX42 and TX10, respectively),

CD300a-human Fc protein and anti-human CD300a (mouse IgG1, TX49) were made in our laboratory, as previously described [55,95]. 1-oleoyl-2-{6-[(7-nitro-2-1,3-benzoxadiazol-4-yl) amino] hexanoyl}-sn-glycero-3-phosphoserine (NBD-PS) was from Avanti. Lipopolysaccharide (LPS; L2880) derived from Escherichia coli O55:B5, ATP (A26209), Ionomycin (I9657) were purchased from Sigma-Aldrich. PSVue480 and PSVue643 were purchased from Molecular Targeting Technologies. Recombinant mouse IL-33 was purchased from R&D (3626-ML).

CD300a-Fc blocking experiment was done with either apoptotic cell induced by dexamethasone or degranulated BMMCs. Briefly, 10^5 cells were incubated with CD300a-Fc together with 50ng anti-CD300a antibody (TX10 or EX42) or 100ng MFG-E8-D89E on ice for 15min, and further stained by anti-CD107a (for BMMCs only) and anti-human IgG Fc-PE (M1310G05, Biolegend) and PI.

Flow cytometry analyses were performed using a LSRFortessa system (BD Bioscience), and data were analyzed by using FlowJo software (BD).

3.3 Degranulation and other stimulations

For mouse in vitro stimulations, MCs were sensitized with 1 μg/ml TNP-specific IgE overnight, washed twice with Tyrode's buffer, pre-incubated with reagents as indicated for 30min, and then challenged with 1ng/ml TNP–OVA for 30min or indicated time point. β-Hexosaminidase activity was measured as previously reported [25]. Briefly, 50 μl of the culture supernatant was mixed with 50 μl of 4-nitorophenyl-N-acetyl-β-D-glucosaminide (1.3 mg/ml; Sigma, N9376) in substrate buffer (0.4 M citric acid, 0.2 M NaH2PO4, pH 4.5) and incubated at 37°C for 3 h. The reaction was stopped by adding 100 μl of glycine (0.2 M, pH 10.7), the solution was thoroughly mixed, and then absorbance of 415 nm was determined. CD107a was measured by flow cytometry after staining with anti-cKit and anti-CD107a

antibodies and PI. Apoptotic thymocytes were induced in 0.2mM dexamethasone with 10^7 cell/ml RPMI medium for 12 hr. Cell density pictures were acquired under 20X objective lens under bright field and converted into binary by ImageJ.

For human MCs stimulation, cultured human synovial MCs were sensitized with 500ng/ml human IgE, stained with 50ug/ml anti-human CD300a or isotype control antibody, challenged with 300ng/ml anti-human IgE antibody for 30min, followed by staining with anti-human CD107a and PI, and analyzed by flow cytometry.

For measuring PS exposure of BMMCs after stimulations by LPS (1 μg/ml), IL-33 (150 ng/ml), TNP-OVA (10 ng/ml), ATP (0.5 mM), or ionomycin (2500 ng/ml), the cells were incubated with indicated reagents for 20 min after IgE sensitization and then stained with antibody against CD107a, annexin V and PI. For measuring degranulation after ATP (0.5mM) or ionomycin (500ng/ml) stimulation, the stimulation time was 30min.

3.4 Live imaging

For time lapse-imaging, BMMCs were sensitized as mentioned above and then incubated in 500 μl of Tyrode's buffer containing 1 mM PSVue-643 fluorescent probe (Polysciences, Inc.) in a glass-bottom dish (CELLview, Greiner Bio-One) for 30 min before gently adding 10 μl of TNP–OVA (100 ng/ml). Cells were monitored under a laser scanning confocal microscope (Olympus FV10i) at 10 s intervals under 60× optical magnification. Data were analyzed and exported by FV10-ASW (Olympus). The video and montage were generated by ImageJ software with 10 frames/s. The confocal images of single mast cells were also collected and analyzed on the same platform with PS stained by PSVue480 and CD300a by Alexa647 conjugated anti-CD300a.

For imaging flow cytometry, the Image Stream Mark II system (Amnis) was used to observe single cells after 15min degranulation and staining. Data were acquired and analyzed by using the Inspire and Ideas software packages (Merck), respectively. The Bright Detail Similarity R3 Feature (based on Pearson correlation coefficient) was adopted as the localization measurement according to the manufacturer's instructions. Briefly, the Bright Detail Similarity R3 Feature value was calculated with a customized imaging mask to identify aggregation of the molecule of interest (CD107a or PS) on the cell surface. To detect colocalization of CD107a and PS, the mask was set on the CD107a channel with the following parameters: Threshold (M05, Ch05, 73) & Peak (M05, Ch05, Bright 10). To detect colocalization of CD300a and PS, the mask was set on the PS channel with following parameters: Threshold (M05, Ch05, 60) & Peak (M05, Ch05, Bright 4). The data were exported as an FCS (Flow Cytometry Standard) file and analyzed by FlowJo (TreeStar).

For FRET analysis, TNP-specific IgE sensitized BMMCs was firstly stained by non-blocking anti-CD300a antibody TX10 (Alexa546 conjugated) for 15min and then labeled by 500nM NBD-PS in Hank's Balanced Salt Solution (HBSS) with 1mM $CaCl_2$ for 8min in room temperature. The cells were immediately washed by 5 mg/ml fatty acid-free Bovine Serum Albumin (BSA) in HBSS with 1mM $CaCl_2$. The stained cells were challenged by TNP-OVA and observed under live imaging conditions with laser set 471nm/559nm and filter set 490nm-540nm and 570nm-620nm.

FRET efficiency was calculated by sensitized emission according to the FRET package instructions in FV10-ASW (Olympus).

$$\text{Efficiency (E)} = 1 - \frac{e}{e + PFRET * \left(\frac{\Psi_{dd}}{\Psi_{aa}}\right) * \left(\frac{Q_d}{Q_a}\right)}$$

Ψ_{dd}, Ψ_{aa}: collection efficiency in donor and acceptor channel;

Q_d, Q_a : Quantum yield of the donor and acceptor;

$$PFRET = f - DSBT - ASBT$$

f: Acceptor with donor excitation

$$DSBT = \left(\frac{b}{a}\right) * e \qquad ASBT = \left(\frac{c}{d}\right) * g$$

e: Donor with donor excitation

g: Acceptor with acceptor excitation

e, f and g were obtained using donor and acceptor double stained samples (FRET samples).

DSBT (donor spectral bleedthrough) and ASBT (acceptor spectral bleedthrough) were calculated by images from the donor/acceptor single stained sample excited by designated laser according to the package instruction to obtain the value *a*, *b c* and *d*. FRET+ cell percentage was calculated by counting the $FRET^+$ cells in each field.

3.5 Phagocytosis assay

8-week old mouse were intraperitoneally injected with 2ml thioglycolate. Four days later, peritoneal cells were harvested by complete DMEM (10% FBS) and seeded in 48-well plate. Wash by warm PBS twice before adding degranulated and stained BMMC.

BMMC were sensitized by TNP-specific IgE for two hours and degranulated with 10ng/ml TNP-OVA in Tyrode's buffer for 10min. After degranulation, BMMC were washed by warm Tyrode's buffer and stained by 100ng/ml pHrodo Red

(ThermoFisher) in HBSS+1mM CaCl2 for 30min RT, followed by wash with complete DMEM (10% FBS). Suspend 10^6 cells/ml in complete DMEM (10% FBS).

Add degranulated and stained BMMC into macrophage wells at 1:1 ratio and incubate for 60min. The reaction was stopped by aspirating the medium and adding 1mM EDTA and incubation for another 10min. Macrophages were detached by pipetting and stained for CD3e-FITC (145-2C11), CD19-FITC (1D3), NK1.1-FITC (PK136), Ly6G-FITC (1A8), KIT-Alexa488 (2B8), F4/80-APC (CI:A3-1), CD11b-APC-Cy7 (M1/70) with 2.4G2 on ice 30min. Phagocytosis was measured by YG-PE^+ cells in lineage $(FITC)^-CD11b^+F4/80^+$ gate.

Apoptotic thymocytes induced by 1μM dexamethasone overnight were used as positive controls.

3.6 Passive systemic anaphylaxis

WT and *Cd300a*$^{-/-}$ mice (age-matched 8- to 14-week-old females) were sensitized by intravenous (i.v.) administration of 5 μg of TNP-specific IgE (BD Biosciences, C38-2) for 24 h and then i.v. challenged with 40 μg TNP–OVA. Body temperature was measured intrarectally at the indicated time points. For antibody blocking, a neutralizing anti-CD300a or isotype (400μg/mice) was injected i.p. 5 h before antigen challenge.

For staining ear tissue sections, 50 μg/mice MFG-E8-D89E (Flag-taged) were i.v injected together with or without 40μg/mice antigen. Ear tissue was harvested 10min after injection and fixed with formalin. Paraffin sections were deparaffinized, antigen retrieval was done by using AR6 buffer (PerkinElmer), staining for MCs by using FITC-Avidin (Biolegend) and PS by using PE-anti-Flag (L5, Biolegend).

3.7 Western blot analysis

One hundred thousand BMMCs were degranulated as described above and immediately washed with ice-cold PBS at the indicated time points. Cells were stimulated with 1 mM sodium orthovanadate and then lysed with 1% (w/v) NP40. The lysates were immunoblotted with antibodies against Syk or phosphorylated Syk.

3.8 Statistical analysis

Statistical analyses were performed using GraphPad Prism software (GraphPad Software). For comparing between two groups, statistical significance was determined by 2-tailed unpaired Student t test with or without correction by Holm-Sidak method. For comparing more than two groups, statistical significance was determined by 2way-ANOVA multiple comparisons with Bonferroni's or Sidak's test. Error bars indicate SEM except for elsewhere mentioned.

4. Results

4.1 Characterization of PS exposure during mast cell degranulation

4.1.1 PS exposure is fast and persistent

To observe PS externalization on the cell surface of viable MCs, we monitored surface PS exposure on TNP-specific IgE sensitized bone marrow-derived cultured MCs (BMMCs) by confocal microscopy during stimulation with TNP-OVA in the presence of PSVue 643, a fluorescent dye with rapid binding capacity for PS. The dye began to accumulate on the cell surface of live BMMCs within 600 s after gentle addition of antigen (FcεRI stimulation), whereas the non-stimulated BMMCs remained negative for the staining (Fig. 2, *A*), indicating that PS is externalized within 10 min after activation.

In the time-laps imaging, antigen reached BMMCs through spontaneous diffusion because antigen addition must minimize the disturbance of the culture to maintain the focus. Therefore, the time after no-mixing antigen addition does not reflect the time after the FcεRI stimulation in the imaging culture. To further investigate the kinetics of PS exposure during degranulation, A quick mixing of antigen and BMMCs was performed immediately after the antigen addition. BMMCs were stimulated for indicated time period and transferred into ice cold Tyrode's buffer to stop the degranulation, then PS exposure along with a degranulation marker - surface CD107a were measured by flow cytometry. As short as 2 mins after FcεRI stimulation, MCs strongly degranulated and externalized PS (Fig. 2, *B*). Different with degranulation marker CD107a, which began to decrease from 8 mins after stimulation, the exposed PS on MCs last for more than 6 hours without significant decay (Fig. 2, *B*). The PS exposure is reversible and disappeared 24 hours after antigen stimulation (Fig. 2, *B*), in consistency with the previous report.

4.1.2 PS exposure is associated with degranulation

MCs can be activated by other non-degranulating stimulations, such as LPS and IL-33; MCs degranulation can also be induced by other stimulators other than FcεRI signaling. We tested PS exposure under different stimulations including non-degranulators LPS and IL-33, and degranulators ATP and inonmycin. Interestingly, PS exposure was observed only under degranulation condition (Fig. 3, *A* and *B*). Both stimulations through TLR-4 by LPS and ST2 by IL-33 failed to induce PS externalization (Fig. 3, *B*). Indeed, the degranulation marker CD107a showed strong colocalization on the degranulated MCs with exposed PS (i.e., $CD107a^+$ Annexin-V^+) as observed by imaging flow cytometry, suggesting that PS exposure on the cell surface of MCs is associated with degranulation (Fig. 3, *B*). Together, these data demonstrate that PS was promptly exposed together with CD107a during degranulation of MCs.

4.1.3 PS^+ MCs after degranulation are not subject to phagocytosis

PS exposure on apoptotic cells serves as an "eat-me" signal for phagocytes engulfment. The relative long-time PS exposure (> 6hrs, Fig. 2, *B*) on stimulated MCs raised a question: Can phagocytes engulf PS^+ live MCs?

To test this possibility, BMMCs were degranulated by FcεRI stimulation and stained with pHrodo, then co-cultured with mouse thioglycolate-induced peritoneal macrophages. No difference of the pHrodo-positive macrophage ($CD11b^+$ $F4/80^+$ gated) population was found between degranulated and non-degranulated MCs, although macrophages did strongly engulf apoptotic cells (Fig. 4). Therefore, PS^+ MCs after degranulation are not subject to phagocytosis.

4.2 Interactions of exposed PS and PS receptor CD300a during MCs degranulation

4.2.1 Co-localization of CD300a and PS during MCs degranulation

To investigate the function of exposed PS during MCs degranulation, we focused on an inhibitory immunoreceptor for PS, CD300a, which is abundantly expressed on MCs. By imaging flow cytometry analysis, we found that both PS and CD300a were polarized and co-localized on the cell surface of mouse BMMCs (Annexin V stained) 15 min after FcεRI stimulation (Fig. 5, *A*). Higher magnification images by confocal microscopy revealed that the colocalized region of PS and CD300a also contained dot-like sub-regions on both mouse BMMCs and cultured human synovial MCs after degranulation (Fig. 5, *B* and *C*).

4.2.2 Interaction of CD300a and PS during MCs degranulation

To measure the direct interaction of CD300a and PS during MCs degranulation, fluorescence resonance energy transfer (FRET) analysis was performed using NBD-PS as a donor and a non-neutralizing anti-CD300a antibody (TX10, Fig. 6, *A*) conjugated with Alexa546 as an acceptor. The fluorescent PS (NBD-PS) was incorporated into MCs by incubation in RT and non-bounded PS was absorbed by 1% BSA. FRET efficiency calculated by sensitized emission between CD300a and PS was increased after degranulation compared with non-stimulated cells (Fig. 6, *B*). Moreover, treatment with a neutralizing anti-CD300a antibody (EX42) that interferes the binding of CD300a with PS (Fig. 6, *A*) dramatically decreased the $FRET^+$ cell number during degranulation (Fig. 6, *C*), demonstrating the direct *cis*-interaction between CD300a and PS in the colocalized region of degranulating MCs. These data suggest that PS externalized during degranulation bound to CD300a on the same MC.

4.3 Functional analysis of PS and CD300a interaction during MCs degranulation *in vitro*

4.3.1 PS-CD300a interaction inhibits MCs degranulation

To examine the functional consequence of *cis*-binding between CD300a and PS, we next examined the degranulation of WT and *Cd300a*$^{-/-}$ BMMCs following stimulation of FcεRI by addition of TNP-specific IgE and TNP–OVA. Flow cytometry analysis showed that the size of the CD107a^{+} population was significantly larger in *Cd300a*$^{-/-}$ BMMCs than in WT BMMCs from 8 min (480 s) to 30 min (1,800 s) after stimulation (Fig. 7, *A* and *B*). Moreover, *Cd300a*$^{-/-}$ BMMCs produced a larger amount of β-hexosaminidase than did WT BMMCs when they were analyzed 30 min after stimulation (Fig. 7, *C*).

Treatment with a neutralizing anti-CD300a antibody (EX42) increased CD107a expression on WT BMMCs to a level comparable to that of *Cd300a*$^{-/-}$ BMMCs (Fig. 7, *D*). Similarly, a neutralizing anti-human CD300a antibody increased the CD107a expression during FcεRI-mediated degranulation of cultured human synovial MCs (Fig. 7, *E*).

Interestingly, FcεRI stimulation also induced a polarization of FcεRI and colocalization of FcεRI with CD300a and PS (Fig. 7, *F, G*). Thus, the same spatio-temporal localization of CD300a, PS and FcεRI on MCs might cause CD300a-mediated suppression of FcεRI-mediated CD107a expression during degranulation. Indeed, Syk phosphorylation was higher in *Cd300a*$^{-/-}$ BMMCs than in WT BMMCs after antigen challenge at 10 min (600 s) after FcεRI stimulation, but was comparable between WT and *Cd300a*$^{-/-}$ BMMCs at 2 min (120 s) after stimulation (Fig. 7, *H*), consistent with our observation that degranulation was significantly higher in *Cd300a*$^{-/-}$ than WT BMMCs at 8 min (480 s), but not 2 min (120 s), after FcεRI stimulation (Fig. 7, *B*). Together, these imaging and functional analyses

indicate that the *cis*-interaction of CD300a with PS suppresses FcεRI-mediated signaling for degranulation of MCs.

4.3.2 PS-CD300a interaction-mediated inhibition of MCs degranulation is cell intrinsic and cell-cell interaction independent

To confirm the cell-intrinsic effect of CD300a on degranulation, equal numbers of WT and *Cd300a*$^{-/-}$ BMMCs were mixed and stimulated with TNP-specific IgE and TNP–OVA. The CD107a^{+} population was again observed to be larger in *Cd300a*$^{-/-}$ BMMCs than in WT BMMCs (Fig. 8, *A* and *B*). We also measured that the population of PI^{+} dead cells were comparable between the cultures of WT and *Cd300a*$^{-/-}$ BMMCs before and after stimulation of FcεRI (Fig. 8*, C*). Moreover, even in the low concentrations of BMMCs in the culture, in which trans-interactions of CD300a with PS were unlikely, *Cd300a*$^{-/-}$ BMMCs still showed increased degranulation compared with WT BMMCs (Fig. 8, *D and E*). These data suggested that the cell-cell interaction-mediated trans-interaction between PS and CD300a had little effect of the inhibitory function of CD300a. Therefore, the inhibitory function of CD300a on FcεRI-mediated MCs degranulation is dependent on *cis*-interaction between self-PS and CD300a.

4.3.3 *cis*-interaction of CD300a with PS specifically suppresses FcεRI-mediated MCs degranulation

To gain insight of CD300a-mediated suppression of MCs degranulation induced by other degranulator other than FcεRI colligation, we visualized BMMCs by staining PS and CD300a after degranulation induction by ATP and ionomycin. Interestingly, although PS was promptly exposed after stimulation, CD300a did not aggregate on the cell surface therefore did not show polarized colocalization with PS (Fig. 9, *A*).

The degranulation measured by CD107a expression was also comparable between WT and *Cd300a*$^{-/-}$ BMMCs (Fig. 9, *B*). These data suggest the inhibition of MCs degranulation mediated by *cis*-interaction of CD300a with PS maybe specific to FcεRI signaling.

4.4 Phenotype of CD300a deficient mice in a MC-dependent PSA model

4.4.1 Impaired recovery of CD300a deficient mice in a passive systemic anaphylaxis model

To investigate the *in vivo* function of CD300a-mediated degranulation suppression, we analyzed the role of CD300a in the pathogenesis of passive systemic anaphylaxis. WT and *Cd300a*$^{-/-}$ mice were i.v. injected with TNP-specific IgE, followed by an i.v. challenge with TNP–OVA. Although rectal temperature of WT and *Cd300a*$^{-/-}$ mice decreased to a similar level by 20 min (1,200 s) after the challenge, the recovery of the rectal temperature after this period was slower in *Cd300a*$^{-/-}$ mice than in WT mice (Fig. 10, *A*), consistent with the time course of the self-regulation of MCs degranulation in vitro by CD300a. Similar results were also observed when mice were i.p. injected with a neutralizing anti-CD300a antibody (EX42) (Fig. 10, *B*), suggesting that the CD300a-PS interaction suppressed PSA.

4.4.2 Involvement of MCs CD300a and PS *cis*-interacting *in vivo* in a PSA model

To investigate the possibility of *cis*-interaction between CD300a and PS on MCs *in vivo* during the course of PSA, Flag-tagged MFG-E8-D89E was intravenously injected together with TNP–OVA and ear tissue was harvested 10 min after the injection. As expected, polarized PS was detected only in the tissue MCs, rather than at regions surrounding MCs, ruling out the possibility of trans-interaction between

CD300a and PS *in vivo*, at least in this model. These results suggest that the *cis*-interaction regulated MCs degranulation *in vitro* as well as *in vivo*.

4.5 CD300a-mediated inhibition of degranulation is a cell-intrinsic feedback mechanism ---- additional evidence from a mathematic modeling approach

To discriminate between the cell-intrinsic and cell-extrinsic mechanism of degranulation inhibition, a system of differential equations was constructed as a simplified mathematical representation of a two-cell interacting system (Fig. 11, *A*). System:

1. The degranulation change of Cell B (DegraB) = IgE signaling of cell B (IgeB) – self decay of degranulation product.

$$\frac{d(\mathrm{DegraB})}{dt} = k1 \times \mathrm{IgeB}(t) - k2 \times \mathrm{DegraB}(t)$$

   Or for degranulation change of Cell A,

$$\frac{d(\mathrm{DegraA})}{dt} = k1 \times \mathrm{IgeA}(t) - k2 \times \mathrm{DegraA}(t)$$

   where, $k1$ is the efficiency of IgE signaling causing degranulation; $k2$ is the self decay rate.

2. The population of mast cell is assumed to be homogenous in response to antigen stimulation.

$$\mathrm{IgeA}(t) = \mathrm{IgeB}(t)$$

3. The Cell A IgE signaling change = intrinsic inhibition from Cell A itself + extrinsic inhibition from Cell B.

$$\frac{d(\mathrm{IgeA})}{dt} = -k4 \times \mathrm{IgeA}(t) - k3 \times \mathrm{DegraB}(t)$$

Or for IgE signaling change of Cell B,

$$\frac{d(\mathrm{IgeB})}{dt} = -k4 \times \mathrm{IgeB}(t) - k3 \times \mathrm{DegraA}(t)$$

where, $k3$ is the extrinsic inhibition efficiency and $k4$ is the intrinsic inhibition efficiency.

In this simplified system, both compromised intrinsic- and extrinsic-inhibition of MC degranulation gave higher degranulation than the normal system before the termination (Fig. 11, *B*). However, system with compromised intrinsic-inhibition, as manipulated by decreased $k4$, terminated the degranulation at similar time point as the Normal system, while system with compromised extrinsic-inhibition, as manipulated by decreased $k3$, had longer time of degranulation and terminated at a later time point than the Normal system (Fig. 11, *B*).

Interestingly, the *Cd300a*$^{-/-}$ BMMCs not only showed increased degranulation before termination, but also terminate the degranulation at a similar time point as WT BMMCs did (Fig. 7, *B* and Fig. 11, *B*), representing traits of the system of compromised intrinsic-inhibition. Therefore, *Cd300a*$^{-/-}$ BMMCs is impaired of cell-intrinsic but not extrinsic inhibition of degranulation, consistent with the notion that PS-CD300a *cis*-interaction-mediated inhibition of MCs degranulation is cell intrinsic and cell-cell interaction independent.

5. Discussion

5.1 *Cis* vs *trans*-interaction and their pathophysiological significance

In current study, we identified a novel regulatory pathway where externalized PS on degranulated MCs serve as a cell-intrinsic negative feedback to down-regulate the degranulation after the onset by binding to an inhibitory receptor CD300a on the same cell, adding another layer of regulation on the MCs degranulation (Fig. 12).

In contrast with previous report, MCs CD300a-mediated inhibition on TLR-4 signaling is dependent on *trans*-interaction between MCs and apoptotic cells in a cecal ligation puncture model of sepsis[19]. Indeed, TLR-4 stimulation did not induce the PS exposure on MCs (Fig. 3, *B*), indicating the distinct ligand origins and requirements of CD300a in different MCs activation condition. As shown in the PSA model, the PS availability for MCs is restricted to itself, suggesting the probable *cis*-interaction between CD300a and PS *in vivo*. Lack of CD300a-PS *cis*-interaction resulted in impaired recovery of body temperature from this PSA model. Although how enhanced MCs degranulation translated into impaired recovery *in vivo* remains intriguing, these results highlight the importance of *cis*-interaction between CD300a and self-PS in the pathogenesis of PSA. Therefore, previous and this study together clearly suggested that the relative importance of *trans*- and *cis*- interaction between receptors and ligands depends on their availability in different pathophysiological situations.

CD300a in this study is an example of *cis*-interaction mediated self-regulation of MCs degranulation. MCs express many other receptors on their cell surface which have regulatory functions on MCs activation while their natural ligands are largely unknow [42,99]. The degranulated MCs may express their ligands on cell surface as the case of CD300a that a chimeric protein of CD300a extracellular

region and human IgG1 constant region (CD300a-Fc) bound to MCs after degranulation (Fig. 6, *A*). Using chimeric protein of other MCs receptors might be able to identify candidates functioning in the similar scenario as CD300a during MCs degranulation.

Importantly, given the rich inflammatory mediator and protease content released after MCs degranulation, MCs activation is a strong immunogenic and maybe disruptive process, therefore should be extensively controlled. However, given that MCs distribution in the tissue in a scattered manner[3], the ligands of its receptors may not be always available without inflammation, highlighting the importance of self-regulatory characteristic of MCs in their activation control.

5.2 PS exposure and recovery

Although PS exposure is a well-established phenomenon after MCs degranulation, the detailed kinetics and characteristics are unknown. In this study, we examined degranulating MCs by live imaging, imaging flow cytometry and flow cytometry with different focus. Live imaging of PS exposure during degranulation identified the PS exposure is minutes-scale event (Fig. 2, *B*) distinct from apoptotic PS exposure, which takes hours to occur[100]. In addition, imaging flow cytometry identified the co-localization of externalized PS and a degranulation marker surface CD107a as well as an inhibitory PS receptor CD300a. Interestingly, the co-localized areas were often polarized on the cell membrane together with IgE receptors (Fig. 3, *B*, Fig. 5, Fig. 7, *F*, *G*), indicating the PS exposure is directly associated with degranulation which happened primarily in the vicinity of the initial FcεRI clusters. The PS^+ area contained both patches-like and dot-like PS^+ regions (Fig. 2 and Fig. 5, *B*), suggesting that the externalized PS may come from different source (e.g. inner leaflet of plasma membrane, membrane of granules and granule itself). These

observations may support the idea that PS is present on the inner membrane of intracellular vesicles (e.g. endosomes or secretory granules)[101].

Exposed PS of apoptotic cell is an "eat-me" signal for macrophages. On the other hand, PS^+ MCs after degranulation cannot be engulfed by phagocytes (Fig. 4), even the PS persisted on the membrane for more than 6 hrs after degranulation (Fig. 2, *B*). Nonetheless, the MCs internalized PS within 24 hrs after degranulation (Fig. 2, *B*) with unknown machinery[94], presumably depend on the flippase activity as evidenced in other types of cell[62]. This MCs specific flippase is of particular interest because flippase mutated cells with stable PS exposure can be engulfed by phagocytes through TAM receptors[87]. A stable PS exposure after MCs degranulation maybe essential for its engulfment by phagocytes[68,73].

5.3 CD300a specificity

CD300a-PS interaction during MCs degranulation showed specific inhibition on FcεRI signaling but not ATP or ionomycin induced degranulation pathways (Fig. 9). In a rat basophilic leukemia cell line, transduced CD300a suppresses FcεRI signaling by phosphatase recruitment through its ITIM motifs[102]. In FcεRI mediated degranulation, Syk phosphorylation is one of the important targets of CD300a (Fig. 7, *H*). It is likely that ATP and ionomycin induced degranulation by causing calcium influx directly into the cytoplasm through activation of cation channels and initiate degranulation without primary requirement of upstream kinase (e.g. Syk) phosphorylation, therefore the inhibitory effect of CD300a was negligible in these situations. In contrast with our observation, another inhibitory receptor of CD300 family, CD300lf, showed modest inhibition of ATP induced MCs degranulation, although the targeted signaling pathway remain elusive[103].

5.4 Technical advances and caveat

5.4.1 PSVue as degranulation monitoring reagent

In this study, we frequently used a small molecule PSVue as a probe for PS detection. The fast binding of PS and PSVue provided a possibility of real-time monitoring of MCs degranulation through its PS exposure. This method is similar with previously reported method using fluorochrome-labeled avidin. Further comparison might be performed to evaluate both methods in parallel.

5.4.2 Protein-lipid FRET

FRET is a sensitive and challenging method frequently used to address protein-protein interactions using FRET parries of fluorescent proteins or fluorophores *in situ*[104]. However, functional interactions in a biological system are not limited to proteins. For example, cells express receptors for lipids (e.g. PS) and carbohydrates (e.g. nuclic? acids). However, FRET technique is rarely used to assess these interactions *in situ*, probably due to lack of proper labeling methods of lipids and carbohydrates.

In current study, we utilized a fluorescent labeled lipid NBD-PS as a FRET donor and non-neutralizing anti-CD300a antibody (TX10, alexa546 conjugated) as an acceptor to perform FRET analysis between CD300a and its natural ligand PS on degranulated MCs. We observed FRET signals (sensitized emission) after MCs degranulation indicating the direct binding of CD300a and its ligand. Moreover, this binding is further confirmed by the dramatic decrease of FRET signals after treatment of a neutralizing antibody against CD300a to block PS binding (Fig. 6, *C*). Although NBD-PS did not represent all the PS in MCs, which probably lead to the underestimation of all the FRET event, this is the first method to measure *in situ* lipid-protein interactions using FRET.

The further modification of this method should consider optimal lipid labeling condition and using fluorescence protein-tagged target protein instead of fluorescence-conjugated antibody.

5.4.3 Mathematical modeling

Our mathematical modeling of MCs degranulation reflects the impacts of cell-intrinsic and extrinsic feedbacks on MCs degranulation process. The system is composed of two cells with three differential equations and is capable of simulate the differential influence of cell-intrinsic and extrinsic feedbacks on the termination of degranulation. It is obvious that the system is over-simplified and further modification of this system should increase the complexity of the signaling networks and cellular components. Nonetheless, current model provides an additional evidence upon our imaging and functional analysis, supporting the cis-interaction between CD300a and PS.

5.5 Future directions

CD300 deficient MCs and mice only showed a modest phenotype in degranulation and PSA, respectively, raising possibility of other candidates participating in the regulation pathway with similar scenario (negative feedback). In addition, Fc protein of certain inhibitory receptors on MCs could bind to degranulated MCs as CD300a-Fc did (data not shown). Therefore, identifying other candidates by strategy described in 5.1 may provide further evidence and the significance of the *cis*-interaction mediated negative-feedback in MCs degranulation regulation.

Other cell types, such as other granulocytes, natural killer cells, cytotoxic T cell and neurons, are also capable of degranulation. The presence of such

degranulation regulatory machinery in other cell types is of great interest and should be systematically investigated.

6. Conclusion

In conclusion, by combining imaging and functional analysis of MCs degranulation, we revealed the physical and functional associations of externalized PS with CD300a via *cis*-interaction on viable MCs during degranulation. Given that MCs are widely distributed in many tissues in a scattered manner without contact each other and apoptotic cells, such self-regulation of MC degranulation represents a novel strategy that MCs evolved to control their own activation, adding another layer of regulation in allergic responses (Fig. 12).

7. Figures

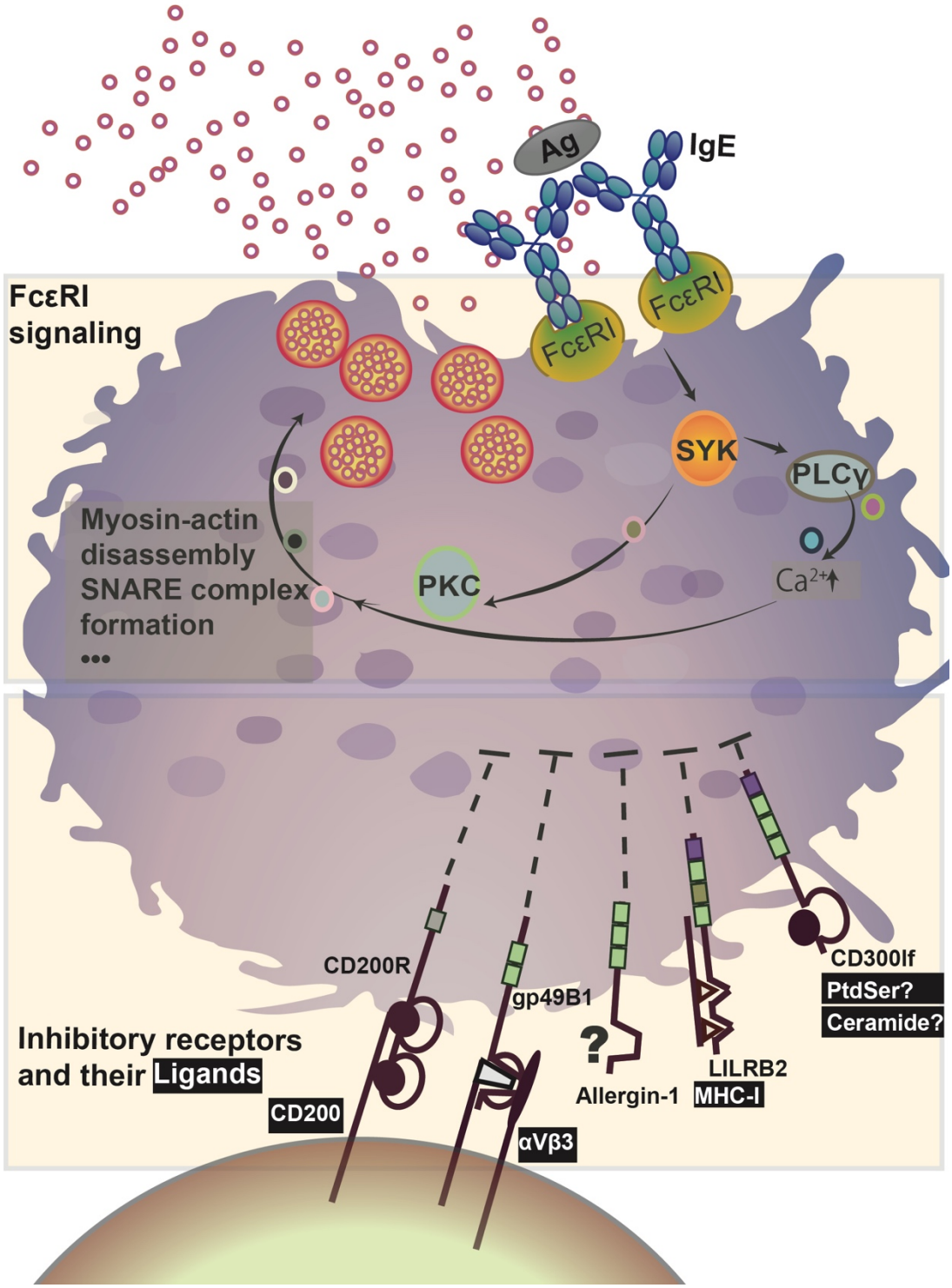

Fig. 1 FcεRI signaling and inhibitory receptors in MCs degranulation.

Cross-linking of FcεRI by antigen drives the phosphorylation of Syk by Src family kinases. Phosphorylated Syk further phosphorylates protein kinase C (PKC) and phospholipase C gamma (PLC γ), resulting in degranulation. The inhibitory

receptors play important yet unclear roles in suppressing degranulation through their interaction with their natural ligands on neighboring cells, MCs itself or not yet identified.

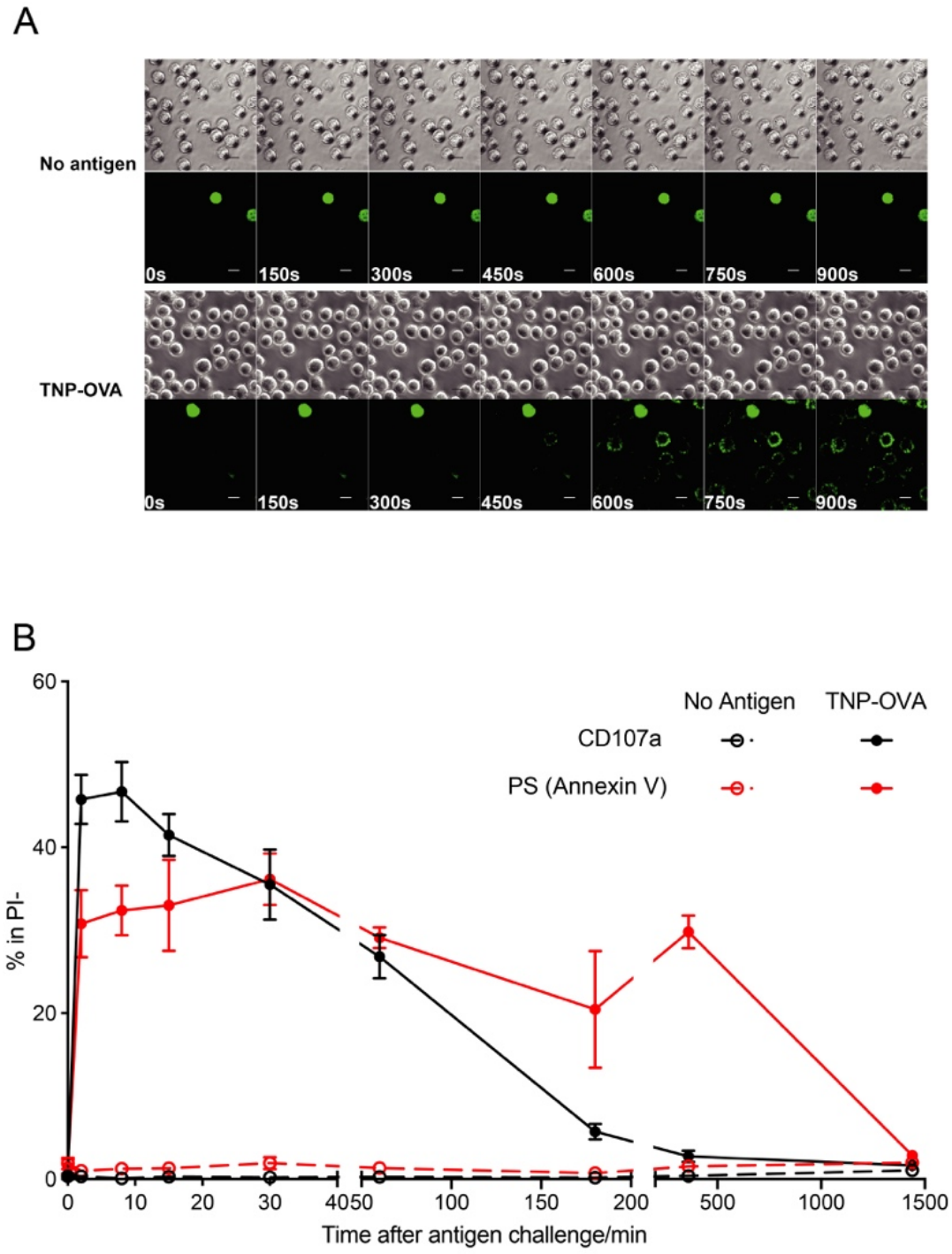

Fig. 2 Kinetics of PS exposure during MCs degranulation

(A) BMMCs were sensitized with TNP-specific IgE and stimulated or not with TNP–OVA in the presence of PSVue643. Time-lapse montage of BMMCs by confocal microscopy shows PS externalization. Dead cells were used as a PSVue-643 staining positive control. Scale bars, 10 μm.

(B) Flow cytometry analysis of cell surface CD107a and PS expression. TNP-specific IgE sensitized BMMC were stimulated or not by 10 ng/ml TNP-OVA for indicated time and stained with CD107a and PSVue on ice then analyzed by flow cytometry.

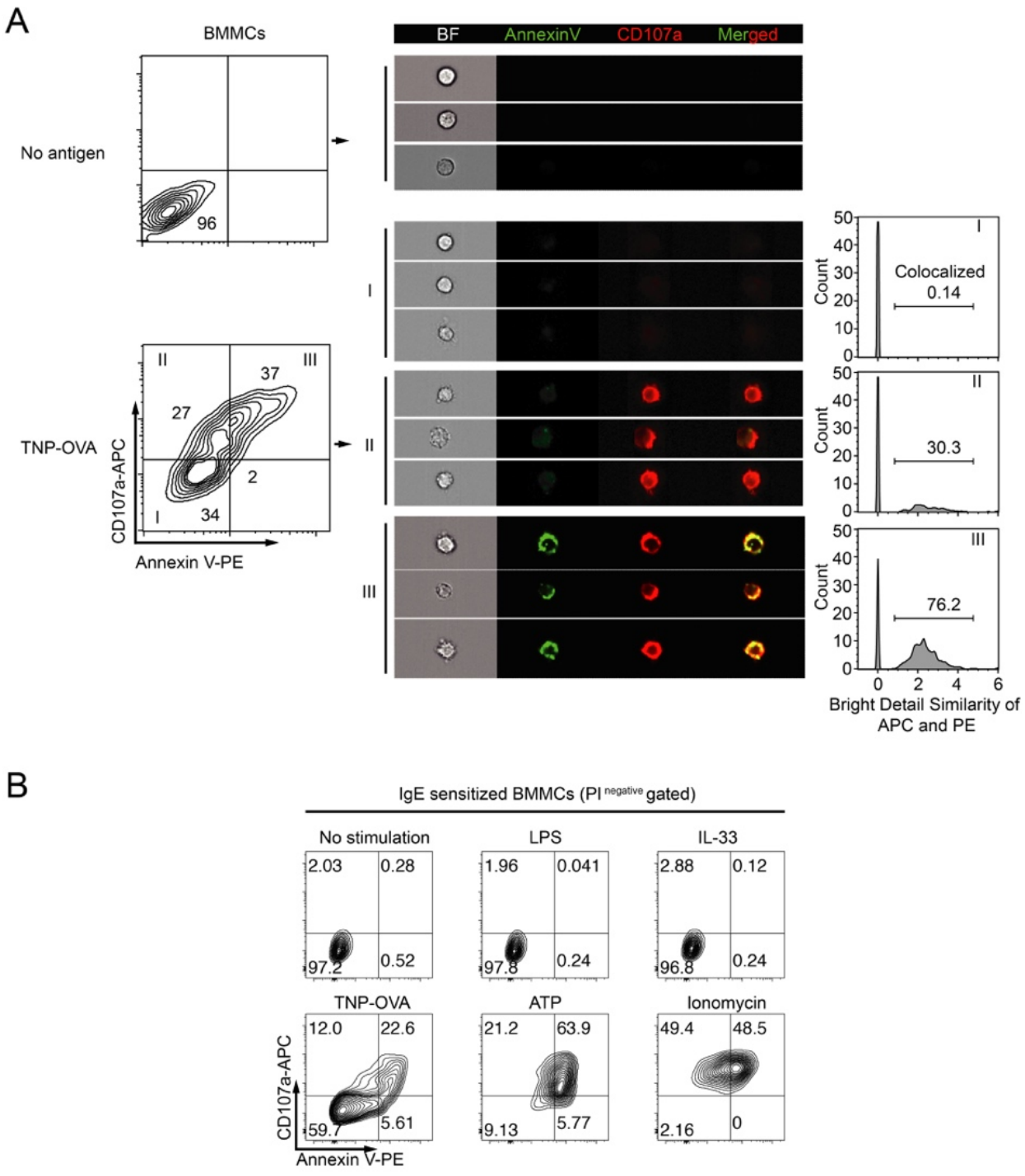

Fig. 3 Characterization of PS exposure during MCs activation

(A) BMMCs were sensitized with TNP-specific IgE, stimulated or not with TNP-OVA for 15 min, stained with anti-CD107a antibody and annexin V, and analyzed by imaging flow cytometry. Representative gating (left) and images of single cells from the gate I, II, and III (middle). Colocalization of CD107a and

PS was analyzed using bright detail similarity R3 based on images of single cells in corresponding gates (right, see section ***3.4***).

(B) BMMCs were sensitized with TNP-specific IgE, stimulated with indicated reagents for 20 min, stained with anti-CD107a, annexin V and PI, and analyzed on the gate of PI^- cells by flow cytometry.

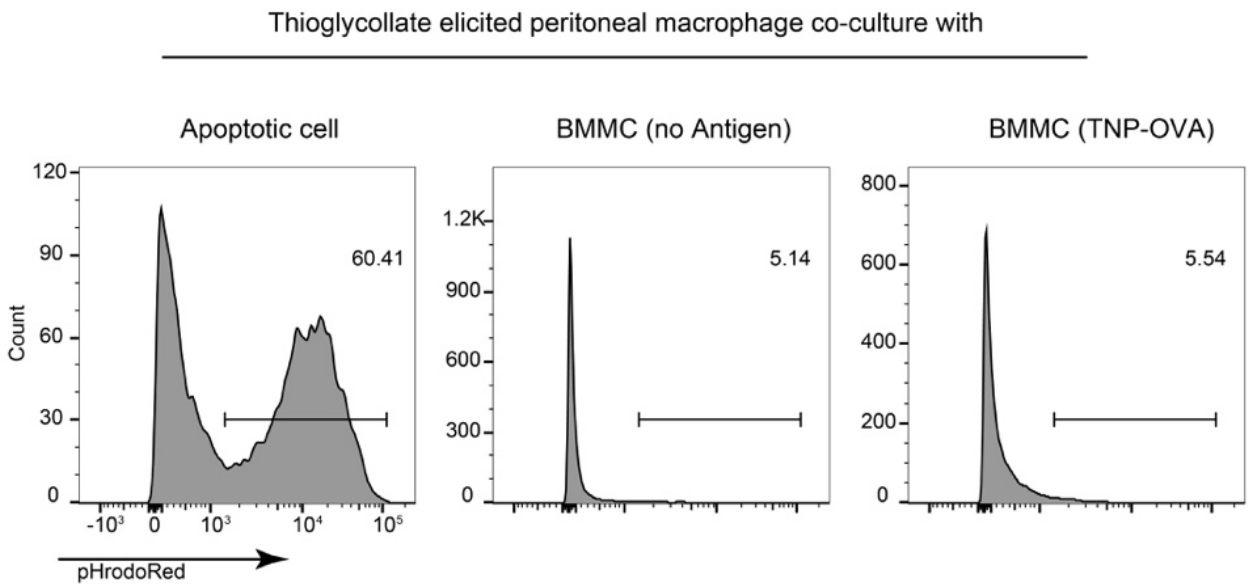

Fig. 4 PS^+ MCs after degranulation are not subject of phagocytosis by macrophage. BMMCs were sensitized with TNP-specific IgE and degranulated or not with 10 ng/ml TNP-OVA, then stained with pHrodoRed, cocultured with peritoneal macrophages for one hour. Macrophages after coculture were detached and live $Lineage^-$ $CD11b^+$ $F4/80^+$ cells were gated for $pHrodo^+$.

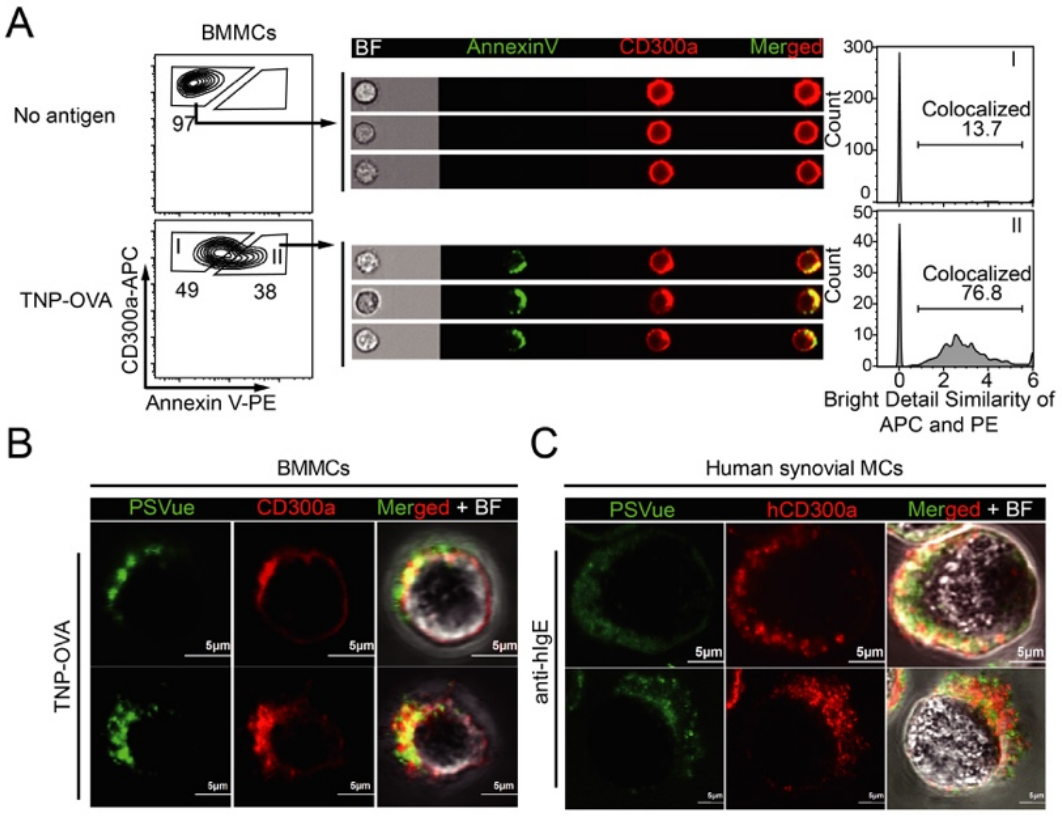

Fig. 5 Localization of PS and PS-receptor CD300a on degranulated MCs

(A) BMMCs were sensitized with TNP-specific IgE and stimulated or not with TNP-OVA for 15 min, then stained with anti-CD300a and annexin V, and analyzed by imaging flow cytometry. Representative gating (left); single cell images (center); and colocalization of CD300a and PS analyzed using bright detail similarity R3 based on images of single cells (see section ***3.4***) in the indicated gate (right).

(B) BMMCs were sensitized with TNP-specific IgE, stimulated or not with TNP-OVA for 15 min, stained with anti-mouse CD300a, and analyzed in the presence of PSVue480 under confocal microscopy.

(C) Cultured human synovial MCs were sensitized with human IgE, stimulated with anti-human IgE or isotype control antibody for 15 min, stained with anti-human CD300a, and analyzed in the presence of PSVue480 under confocal microscopy.

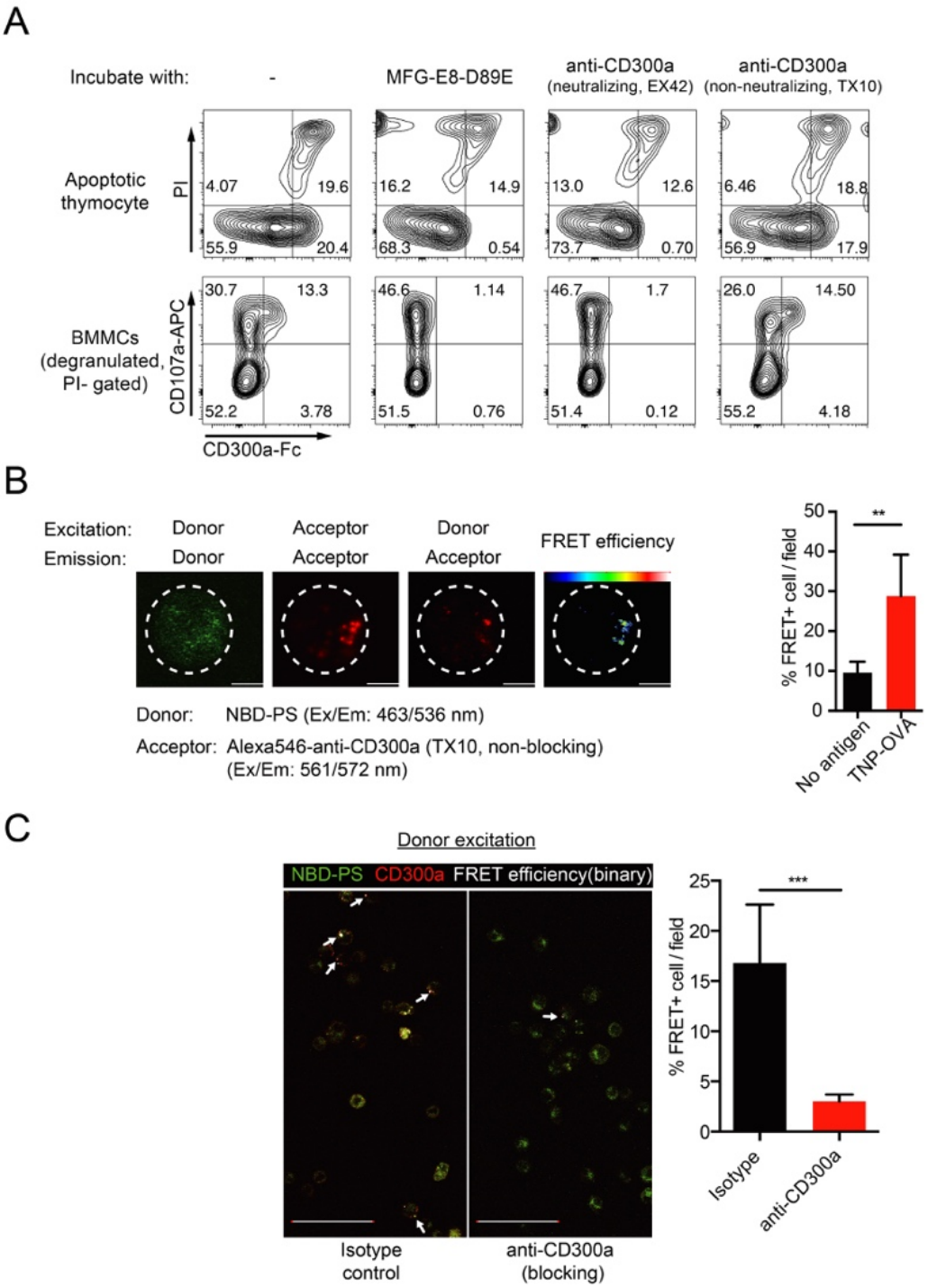

Fig. 6 FRET measurement between CD300a and PS

(A) Apoptotic mouse thymocytes induced by treatment with dexamethasone or degranulating BMMCs induced by antigen stimulation were incubated with MFG-E8-D89E, neutralizing anti-mouse CD300a (EX42), or non-neutralizing anti-mouse CD300a (TX10) together with chimeric mouse CD300a-Fc, followed

by an PE-conjugated antibody against human IgG and PI, in the presence of $CaCl_2$, and analyzed by flow cytometry.

(B) BMMC was sensitized with TNP-specific IgE, labeled with NBD-PS and non-neutralizing anti-CD300a antibody (TX10, alexa546 labeled) and stimulated by TNP-OVA. FRET analysis between CD300a and PS: representative confocal pictures (left) and $FRET^+$ cell quantification (right) (see section ***3.4***). Scale bars, 5 μm. Error bars indicate SD.

(C) FRET analysis of the CD300a-PS interaction on BMMCs as in (B) except that the cells were pretreated with either isotype or anti-CD300a neutralizing antibody during degranulation. Representative merged image (left) and $FRET^+$ cell quantification (right). White arrows indicate $FRET^+$ cells. Scale bars, 50 μm.

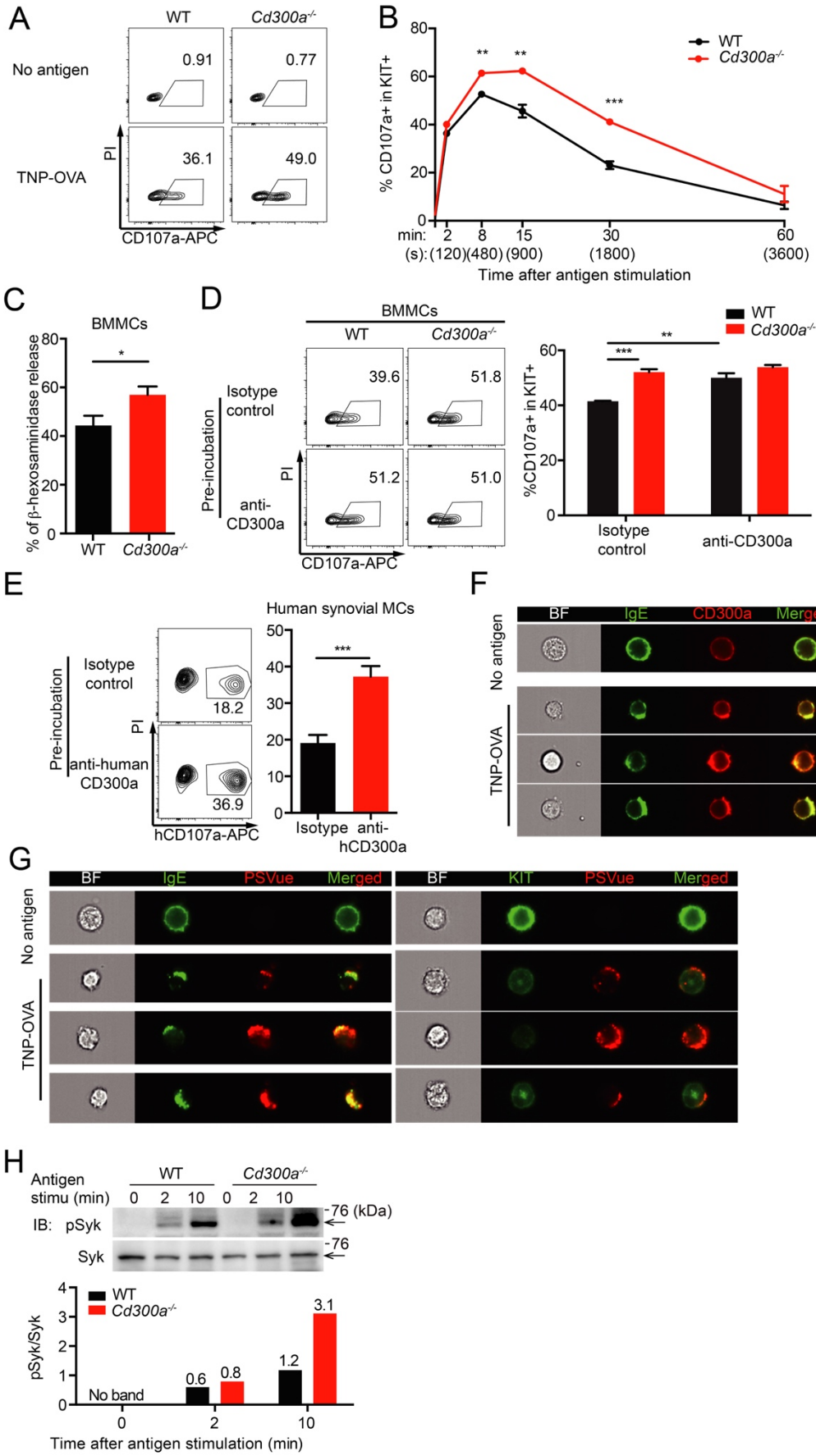
A
WT
Cd300a-/-
No antigen
0.91
0.77
TNP-OVA
36.1
49.0
PI
CD107a-APC
B
% CD107a+ in KIT+
WT
Cd300a-/-
**
**
***
min: 2 8 15 30 60
(s): (120) (480) (900) (1800) (3600)
Time after antigen stimulation
C
BMMCs
% of β-hexosaminidase release
*
WT
Cd300a-/-
D
BMMCs
WT
Cd300a-/-
Isotype control
anti-CD300a
Pre-incubation
39.6
51.8
51.2
51.0
PI
CD107a-APC
%CD107a+ in KIT+
***
**
Isotype control
anti-CD300a
E
Human synovial MCs
Isotype control
anti-human CD300a
Pre-incubation
18.2
36.9
PI
hCD107a-APC
***
Isotype
anti-hCD300a
F
BF
IgE
CD300a
Merged
No antigen
TNP-OVA
G
BF
IgE
PSVue
Merged
BF
KIT
PSVue
Merged
No antigen
TNP-OVA
H
Antigen stimu (min)
WT
Cd300a-/-
0 2 10 0 2 10
IB: pSyk
-76 (kDa)
Syk
-76
WT
Cd300a-/-
pSyk/Syk
No band
0.6
0.8
1.2
3.1
0 2 10
Time after antigen stimulation (min)

Fig. 7 Functional interaction between CD300a and PS externalized during degranulation of MCs

(**A-C**) WT or *Cd300a*$^{-/-}$ BMMCs were sensitized with TNP-specific IgE and stimulated or not with TNP–OVA for 30 min (**A**, **C**) or the indicated time (**B**).

(A) Representative plots showing CD107a expression on the gate of PI^{-} c-Kit^{+} cells.

(B) Kinetics of CD107a expression after antigen stimulation.

(C) β-hexosaminidase release in the culture after degranulation.

(D) WT and *Cd300a*$^{-/-}$ BMMCs were sensitized with anti-TNP IgE and pretreated with a neutralizing anti-CD300a antibody or control antibody, followed by challenge with TNP-OVA antigen. BMMCs were then analyzed for CD107a expression on the gate of PI^{-} c-Kit^{+} cells by flow cytometry.

(E) Cultured human synovial MCs were sensitized with human IgE and pretreated with a neutralizing anti-human CD300a antibody or control antibody, followed by challenge with anti-human IgE, and then analyzed for CD107a expression by flow cytometry on the gate of PI^{-} c-Kit^{+} cells by flow cytometry.

(F, G) BMMCs were sensitized with TNP-specific IgE, challenged or not with TNP-OVA antigen for 15 min, then stained with anti-IgE and anti-CD300a antibodies (F), or PSVue643 plus either anti-IgE or anti-cKit (G), and analyzed by imaging flow cytometry.

(H) Western blot analysis of Syk phosphorylation in whole cell lysates of degranulated WT and *Cd300a*$^{-/-}$ BMMCs at indicated time points. The relative amount of phosphorylated Syk, as determined by densitometry, before and after stimulation is also shown. Data are representative of two independent experiments.

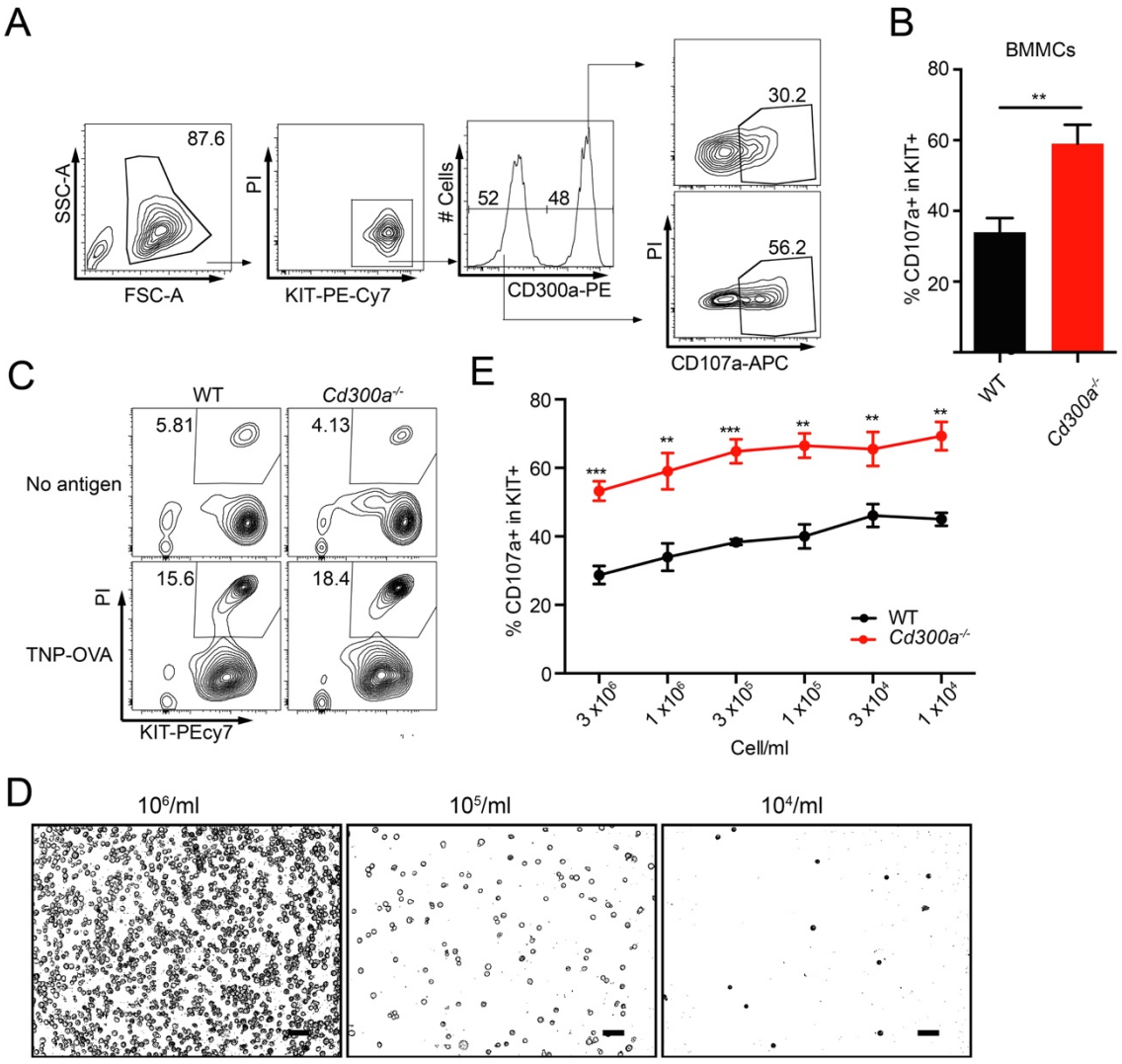

Fig. 8 Increased degranulation in *Cd300a*$^{-/-}$ BMMCs is cell intrinsic and independent of cell-cell interaction

(A, B) WT and *Cd300a*$^{-/-}$ BMMCs were equally mixed and sensitized with TNP-specific IgE, stimulated with TNP–OVA for 30 min, stained with antibodies against CD107a, c-Kit, and CD300a and PI and analyzed by flow cytometry. Data are representative plots (A) and the mean CD107a expression (B) showing in WT and *Cd300a*$^{-/-}$ BMMCs.

(C) WT and *Cd300a*$^{-/-}$ BMMCs were sensitized with anti-TNP IgE, challenged with TNP-OVA for 30 min, stained with anti-c-Kit and PI, and analyzed by flow cytometry.

(D, E) WT and *Cd300a*$^{-/-}$ BMMCs were sensitized with anti-TNP IgE, diluted into different density (scale 50μm) (D), and then challenged with TNP-OVA for 30 min. BMMCs were then stained with antibodies against CD107a and c-Kit and PI, analyzed by flow cytometry (E).

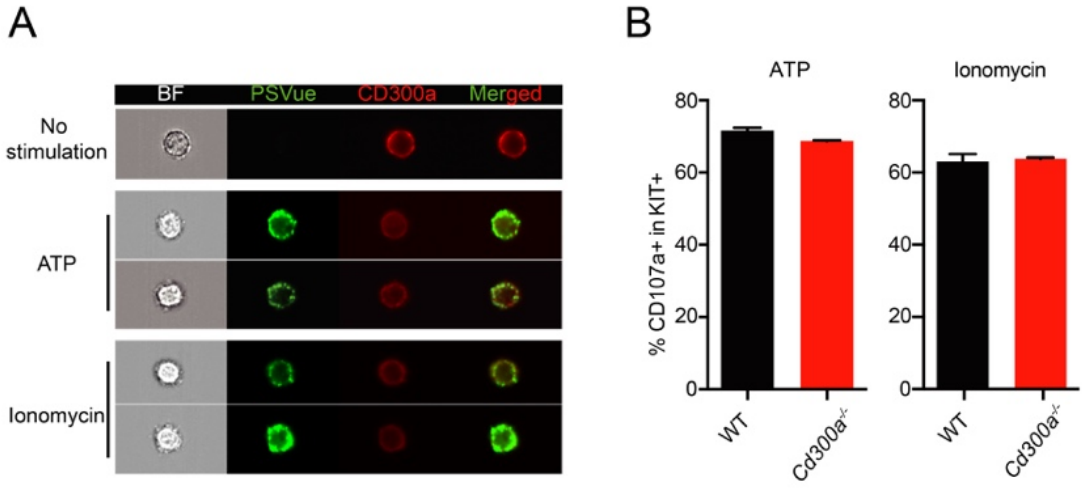

Fig. 9 ATP and ionomycin induced MCs degranulation

(A) BMMCs were sensitized with TNP-specific IgE, stimulated with indicated reagents for 20 min, stained with anti-CD300a antibody and PSVue643, and analyzed by imaging flow cytometry.

(B) WT and *Cd300a*$^{-/-}$ BMMCs were stimulated with 0.5 mM ATP or 500 ng/ml ionomycin, stained with anti-CD107a, anti-cKit and PI, analyzed by flow cytometry.

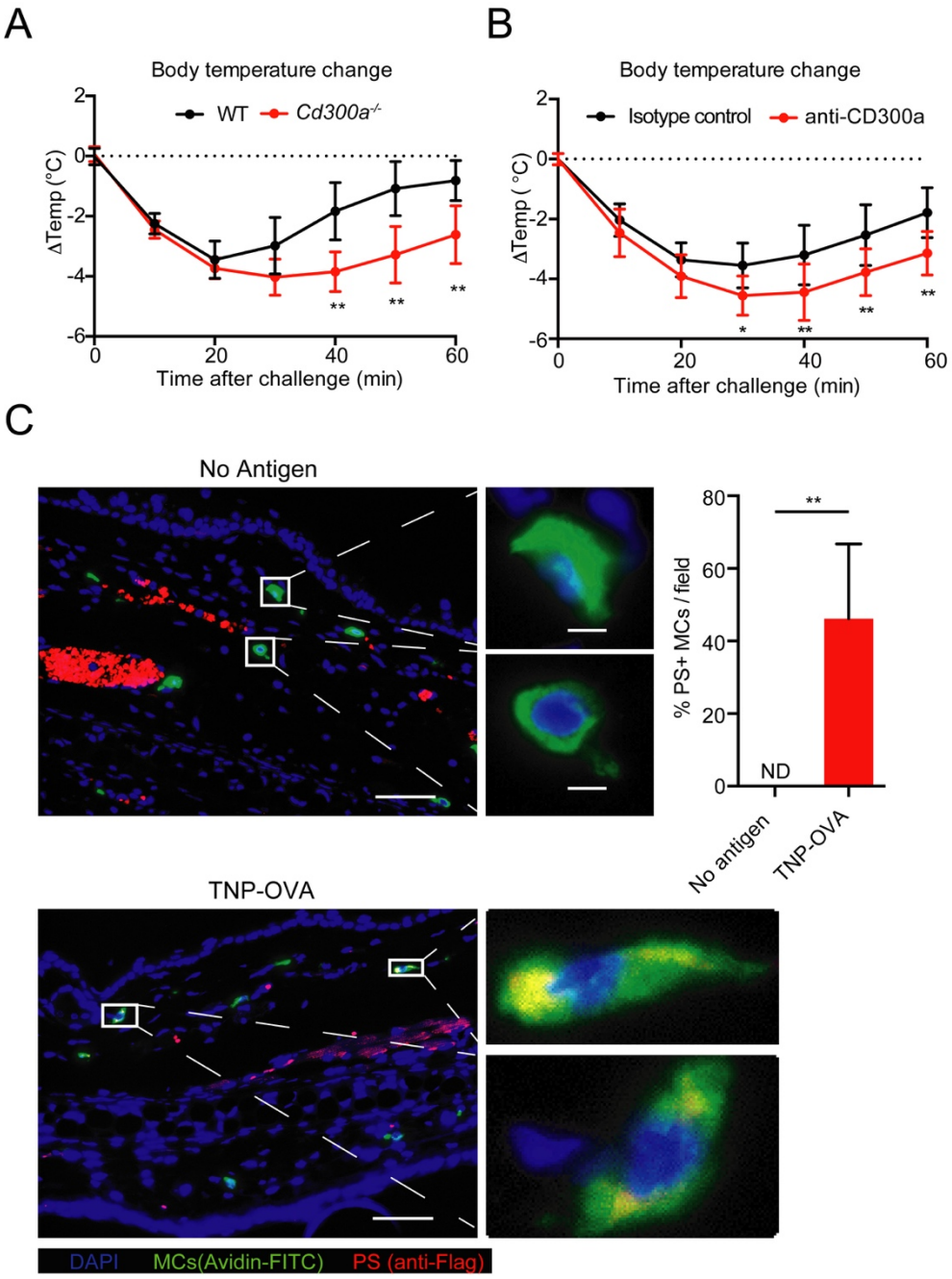

Fig. 10 Involvement of CD300a-PS *cis*-interaction in a PSA model.

(A) Change in intrarectal temperature in WT (n = 6) and *Cd300a*$^{-/-}$ (n = 6) mice after i.v. sensitization with TNP-specific IgE, followed by i.v. challenge with TNP–OVA. Data are pooled from two experiments and error bars indicate SD.

(B) Change in intrarectal temperature in mice injected i.p. with control (n = 8) or anti-CD300a (n = 9) antibody after i.v. sensitization with TNP-specific IgE,

followed by i.v. challenge with TNP–OVA. Data are pooled from three experiments and error bars indicate SD.

(C) Immunohistochemistry analysis of PS exposure in MCs during PSA. WT mice were sensitized with TNP-specific IgE 24hr before injection of 50 μg MFG-E8-D89E (Flag-taged) together with or without 40 μg TNP-OVA antigen. Ten min after the injection, ear tissue sections were stained for MCs by FITC-conjugated Avidin and for PS by PE-conjugated anti-Flag antibody. Scale bars: 50 μm (tissue view) and 5 μm (enlarged cell view).

A

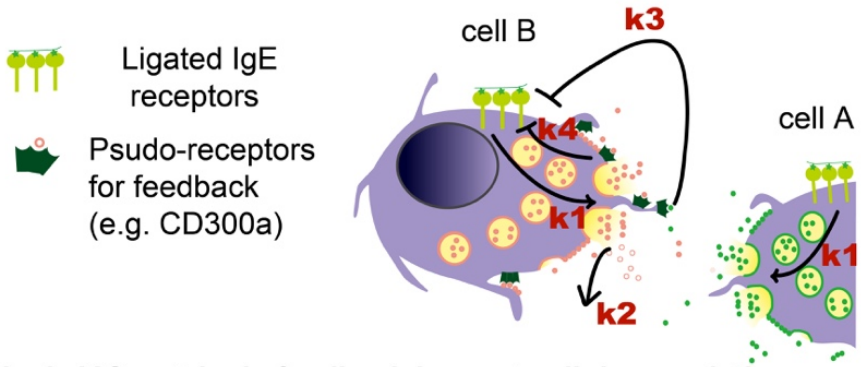

B

Intrinsic V.S. extrinsic feedback in mast cell degranulation

System

1. degraB'[t] = k1*IgeB[t]- k2*degraB[t]

OR: degraA'[t] = k1*IgeA[t]- k2*degraA[t]

Cell B degranulation change=IgE signal -degranulation products self decay

2. IgeA[t]=IgeB[t]

The population of mast cell is assumed to be homogenous in response to antigen stimulation

3. IgeA'[t] = -k4*IgeA[t]-k3*degraB[t]

OR: IgeB'[t] = -k4*IgeB[t]-k3*degraA[t]

Cell A IgE signal change == Cell A intrinsic inhibition + Cell B extrinsic inhibition

Parameter used in modeling by Mathematica NDSolve

InitialConditions: Ige[0] = 10; deg[0] = 0

	Compromized intrinsic	Normal	Compromized extrinsic
k1	0.55	0.55	0.55
k2	2	2	2
k3	2	2	0
k4	0.8	1	1

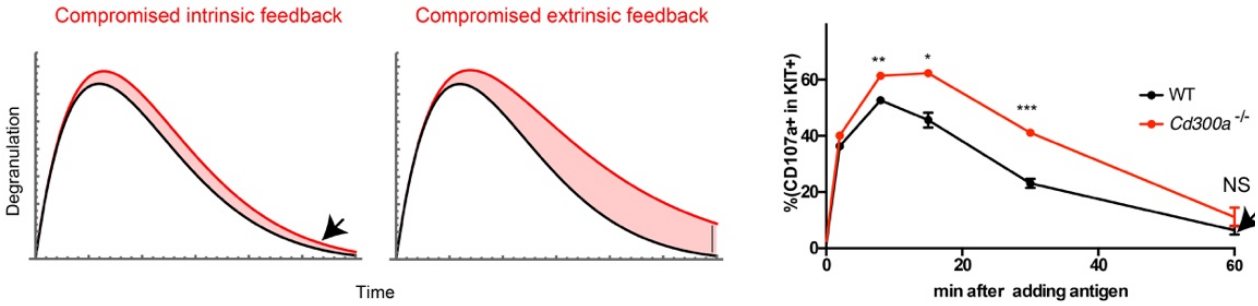

Fig. 11 Mathematical modeling of MCs degranulation with intrinsic and extrinsic feedback regulation

(A) Graphical representation of the two-cell model.

(B) System, parameters and results of the model in comparison of experimental data.

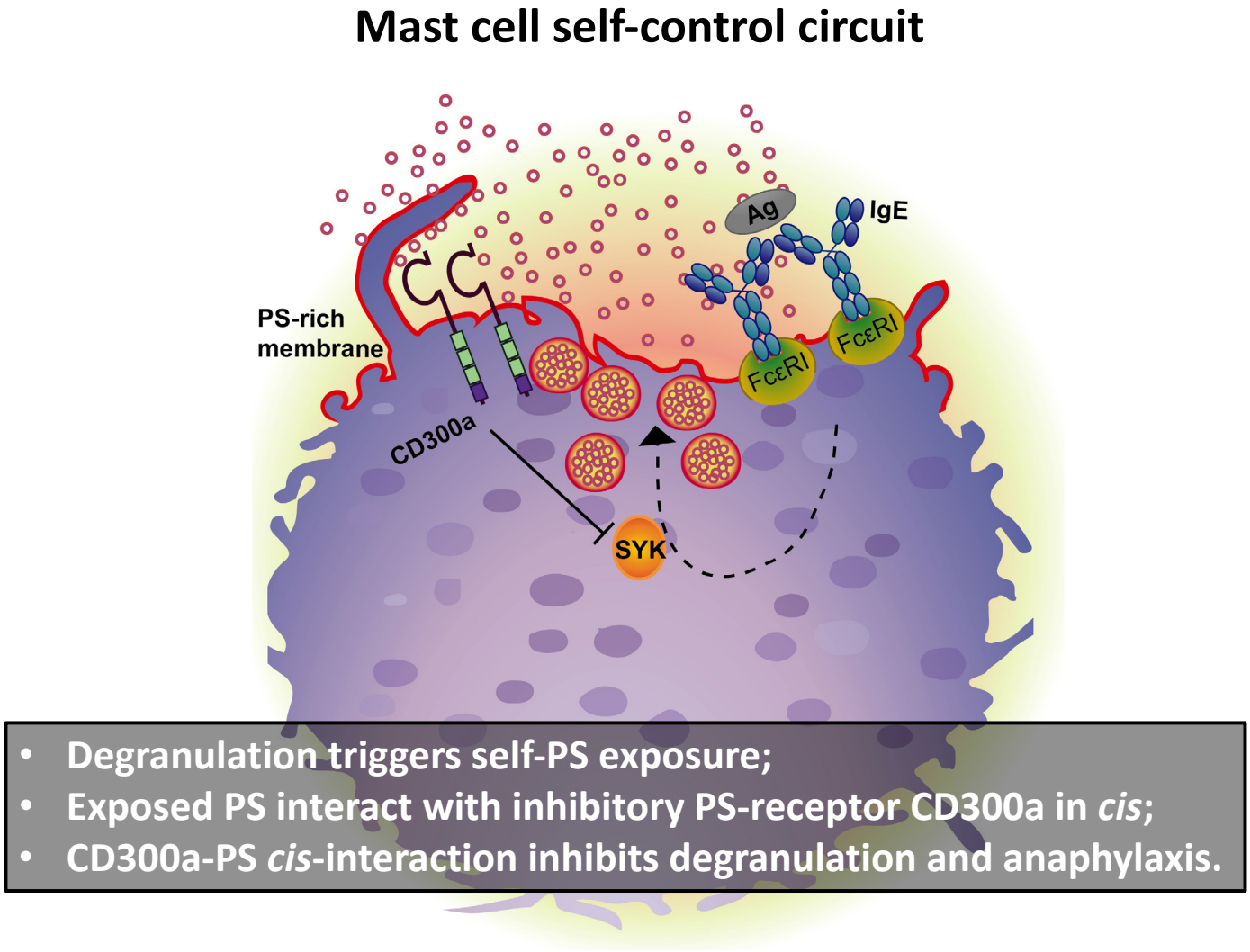

Fig. 12 Graphical summary

8. Reference

1. Baccari, G., Pinelli, C., Santillo, A., Minucci, S. & Rastogi, R. International Review of Cell and Molecular Biology. *Int Rev Cel Mol Bio* **290,** 1–53 (2011).

2. Welle, M. Development, significance, and heterogeneity of mast cells with particular regard to the mast cell-specific proteases chymase and tryptase. *Journal of Leukocyte Biology* **61,** 233–245 (1997).

3. Irani, A., hechter, N., Craig, S., DeBlois, G. & Schwartz, L. Two types of human mast cells that have distinct neutral protease compositions. *Proceedings of the National Academy of Sciences of the United States of America* **83,** 4464–8 (1986).

4. Beaven, M. A. Our perception of the mast cell from Paul Ehrlich to now. *European Journal of Immunology* **39,** 11–25 (2009).

5. Moon, T. *et al.* Advances in mast cell biology: new understanding of heterogeneity and function. *Mucosal Immunology* **3,** mi2009136 (2009).

6. Cass, R., Riley, J., West, G., Head, K. & Stroud, S. Heparin and Histamine in Mast-Cell Tumours from Dogs. *Nature* **174,** 174318b0 (1954).

7. Riley, J. & West, G. Histamine in tissue mast cells. *J Physiology* **117,** 72P-73P (1952).

8. Riley, J. & West, G. The presence of histamine in tissue mast cells. *J Physiology* **120,** 528–537 (1953).

9. Ishizaka, K. & Ishizaka, T. Identification of gamma-E-antibodies as a carrier of reaginic activity. *Journal of immunology (Baltimore, Md. : 1950)* **99,** 1187–98 (1967).

10. Ishizaka, K. & Ishizaka, T. Physicochemical properties of reaginic antibody I. Association of reaginic activity with an immunoglobulin other than γA- or γG-globulin. *J Allergy* **37,** 169–185 (1966).

11. Barsumian, E. L., Isersky, C., Petrino, M. G. & Siraganian, R. P. IgE-induced histamine release from rat basophilic leukemia cell lines: isolation of releasing and

nonreleasing clones. *European Journal of Immunology* **11,** 317–323 (1981).

12. Kulczycki, A., Isersky, C. & Metzger, H. The Interaction of IgE with Rat Basophilic Leukemia Cells I. Evidence for Specific Binding of IgE. *The Journal of Experimental Medicine* **139,** 600–616 (1974).

13. Blank, U. *et al.* Complete structure and expression in transfected cells of high affinity IgE receptor. *Nature* **337,** 337187a0 (1989).

14. Moon, T., Befus, D. A. & Kulka, M. Mast Cell Mediators: Their Differential Release and the Secretory Pathways Involved. *Frontiers in Immunology* **5,** (2014).

15. Mukai, K., Tsai, M., Saito, H. & Galli, S. J. Mast cells as sources of cytokines, chemokines, and growth factors. *Immunological Reviews* **282,** 121–150 (2018).

16. Johnzon, C.-F., Rönnberg, E. & Pejler, G. The Role of Mast Cells in Bacterial Infection. *The American Journal of Pathology* **186,** 4–14 (2016).

17. Nardo, A., Yamasaki, K., Dorschner, R. A., Lai, Y. & Gallo, R. L. Mast Cell Cathelicidin Antimicrobial Peptide Prevents Invasive Group A Streptococcus Infection of the Skin. *The Journal of Immunology* **180,** 7565–7573 (2008).

18. Mekori, Y. A. & Metcalfe, D. D. Mast cells in innate immunity. *Immunological Reviews* **173,** 131–140 (2000).

19. Nakahashi-Oda, C. *et al.* Apoptotic cells suppress mast cell inflammatory responses via the CD300a immunoreceptor. *The Journal of experimental medicine* **209,** 1493–503 (2012).

20. Galli, S. J., Nakae, S. & Tsai, M. Mast cells in the development of adaptive immune responses. *Nature Immunology* **6,** 135–142 (2005).

21. Feyerabend, T. B. *et al.* Cre-Mediated Cell Ablation Contests Mast Cell Contribution in Models of Antibody- and T Cell-Mediated Autoimmunity. *Immunity* **35,** 832–844 (2011).

22. Grimbaldeston, M. A. *et al.* Mast cell-deficient W-sash c-kit mutant Kit W-

sh/W-sh mice as a model for investigating mast cell biology in vivo. *The American journal of pathology* **167,** 835–48 (2005).

23. Yagi, R., Tanaka, S., Motomura, Y. & Kubo, M. Regulation of the Il4 Gene Is Independently Controlled by Proximal and Distal 3' Enhancers in Mast Cells and Basophils. *Molecular and Cellular Biology* **27,** 8087–8097 (2007).

24. Strait, R. T., Morris, S. C., Yang, M., Qu, X.-W. & Finkelman, F. D. Pathways of anaphylaxis in the mouse. *Journal of Allergy and Clinical Immunology* **109,** 658–668 (2002).

25. Hitomi, K. *et al.* An immunoglobulin-like receptor, Allergin-1, inhibits immunoglobulin E–mediated immediate hypersensitivity reactions. *Nature Immunology* **11,** ni.1886 (2010).

26. Kraft, S. *et al.* The Tetraspanin CD63 Is Required for Efficient IgE-Mediated Mast Cell Degranulation and Anaphylaxis. *The Journal of Immunology* **191,** 2871–2878 (2013).

27. Wang, M. *et al.* Peanut-induced intestinal allergy is mediated through a mast cell–IgE–FcεRI–IL-13 pathway. *Journal of Allergy and Clinical Immunology* **126,** 306-316.e12 (2010).

28. Ushio, H. *et al.* Crucial role for autophagy in degranulation of mast cells. *Journal of Allergy and Clinical Immunology* **127,** 1267-1276. e6 (2011).

29. Abbas, A. K., Lichtman, A. H. & Shiv. *Cellular and Molecular Immunology*. *Elsevier* (Elsevier).

30. Lagunoff, D. & Benditt, E. P. Mast Cell Degranulation and Histamine Release Observed in a New *in vitro* System. *The Journal of Experimental Medicine* **112,** 571–580 (1960).

31. Mazingue, C., Dessaint, J.-P. & Capron, A. [3H] serotonin release: An improved method to measure mast cell degranulation. *Journal of Immunological Methods* **21,**

65–77 (1978).

32. Razin, E. *et al.* IgE-mediated release of leukotriene C4, chondroitin sulfate E proteoglycan, beta-hexosaminidase, and histamine from cultured bone marrow-derived mouse mast cells. *The Journal of Experimental Medicine* **157,** 189–201 (1983).

33. Grützkau, A. *et al.* LAMP-1 and LAMP-2, but not LAMP-3, are reliable markers for activation-induced secretion of human mast cells. *Cytometry Part A* **61A,** 62–68 (2004).

34. Kawakami, T. *et al.* Deficient Autophagy Results in Mitochondrial Dysfunction and FSGS. *Journal of the American Society of Nephrology* **26,** 10401052 (2014).

35. Xiao, W. *et al.* Positive and negative regulation of mast cell activation by Lyn via the FcεRI. *The Journal of Immunology* **175,** 6885–6892 (2005).

36. Odom, S. *et al.* Negative Regulation of Immunoglobulin E–dependent Allergic Responses by Lyn Kinase. *J Exp Medicine* **199,** 1491–1502 (2004).

37. Nishizumi, H. & Yamamoto, T. Impaired tyrosine phosphorylation and Ca2+ mobilization, but not degranulation, in lyn-deficient bone marrow-derived mast cells. *The Journal of Immunology* **158,** 2350–2355 (1997).

38. Hernandez-Hansen, V. *et al.* Dysregulated FcεRI Signaling and Altered Fyn and SHIP Activities in Lyn-Deficient Mast Cells. *J Immunol* **173,** 100–112 (2004).

39. Zhang, J., Berenstein, E., Evans, R. & Siraganian, R. Transfection of Syk protein tyrosine kinase reconstitutes high affinity IgE receptor-mediated degranulation in a Syk-negative variant of rat basophilic leukemia RBL-2H3 cells. *The Journal of Experimental Medicine* **184,** 71–79 (1996).

40. Wang, D. *et al.* Phospholipase Cγ2 Is Essential in the Functions of B Cell and Several Fc Receptors. *Immunity* **13,** 25–35 (2000).

41. Finkelman, F. D. Anaphylaxis: Lessons from mouse models. *Journal of Allergy*

and Clinical Immunology **120,** 506–515 (2007).

42. Bulfone-Paus, S., Nilsson, G., Draber, P., Blank, U. & Levi-Schaffer, F. Positive and Negative Signals in Mast Cell Activation. *Trends in Immunology* **38,** 657–667 (2017).

43. Galli, S. J. *et al.* Mast cells as "tunable" effector and immunoregulatory cells: recent advances. *Annu Rev Immunol* **23,** 749–786 (2005).

44. Gilfillan, A. M. & Rivera, J. The tyrosine kinase network regulating mast cell activation. *Immunological Reviews* **228,** 149–169 (2009).

45. Molderings, G. J. *et al.* Pharmacological treatment options for mast cell activation disease. *Naunyn-Schmiedeberg's Archives of Pharmacology* **389,** 671–694 (2016).

46. Föger, N. *et al.* Differential regulation of mast cell degranulation versus cytokine secretion by the actin regulatory proteins Coronin1a and Coronin1b. *The Journal of Experimental Medicine* **208,** 1777–1787 (2011).

47. Lorentz, A., Baumann, A., Vitte, J. & Blank, U. The SNARE Machinery in Mast Cell Secretion. *Frontiers in Immunology* **3,** 143 (2012).

48. Metcalfe, D. D., Peavy, R. D. & Gilfillan, A. M. Mechanisms of mast cell signaling in anaphylaxis. *Journal of Allergy and Clinical Immunology* **124,** 639–646 (2009).

49. Baker, R. W. & Hughson, F. M. Chaperoning SNARE assembly and disassembly. *Nat Rev Mol Cell Bio* **17,** 465–479 (2016).

50. Kneussel, M. & Wagner, W. Myosin motors at neuronal synapses: drivers of membrane transport and actin dynamics. *Nat Rev Neurosci* **14,** 233 (2013).

51. Robbie-Ryan, M., Tanzola, M. B., Secor, V. H. & Brown, M. A. Cutting edge: both activating and inhibitory Fc receptors expressed on mast cells regulate experimental allergic encephalomyelitis disease severity. *Journal of immunology*

(Baltimore, Md. : 1950) **170,** 1630–4 (2003).

52. Katz, H. *et al.* Mouse mast cell gp49B1 contains two immunoreceptor tyrosine-based inhibition motifs and suppresses mast cell activation when coligated with the high-affinity Fc receptor for IgE. *Proceedings of the National Academy of Sciences of the United States of America* **93,** 10809–14 (1996).

53. Liénard, H., Bruhns, P., Malbec, O., Fridman, W. & ëron. Signal regulatory proteins negatively regulate immunoreceptor-dependent cell activation. *The Journal of biological chemistry* **274,** 32493–9 (1999).

54. Masuda, A., Nakamura, A., Maeda, T., Sakamoto, Y. & Takai, T. Cis binding between inhibitory receptors and MHC class I can regulate mast cell activation. *The Journal of Experimental Medicine* **204,** 907–920 (2007).

55. Yotsumoto, K. *et al.* Paired Activating and Inhibitory Immunoglobulin-like Receptors, MAIR-I and MAIR-II, Regulate Mast Cell and Macrophage Activation. *The Journal of Experimental Medicine* **198,** 223–233 (2003).

56. Yamanishi, Y. *et al.* A soluble form of LMIR5/CD300b amplifies lipopolysaccharide-induced lethal inflammation in sepsis. *Journal of immunology (Baltimore, Md. : 1950)* **189,** 1773–9 (2012).

57. Izawa, K. *et al.* The Receptor LMIR3 Negatively Regulates Mast Cell Activation and Allergic Responses by Binding to Extracellular Ceramide. *Immunity* **37,** 827–839 (2012).

58. Cooper, G. *The Cell - A Molecular Approach 2nd Edition*. *The Cell - A Molecular Approach 2nd Edition* (Sunderland (MA): Sinauer Associates).

59. van Meer, G., Voelker, D. R. & Feigenson, G. W. Membrane lipids: where they are and how they behave. *Nature Reviews Molecular Cell Biology* **9,** 112–124 (2008).

60. van Meer, G. & de Kroon, A. Lipid map of the mammalian cell. *Journal of Cell*

Science **124,** 5–8 (2011).

61. igneuret & Devaux, P. ATP-dependent asymmetric distribution of spin-labeled phospholipids in the erythrocyte membrane: relation to shape changes. *Proceedings of the National Academy of Sciences* **81,** 3751–3755 (1984).

62. Nagata, S. Apoptosis and Clearance of Apoptotic Cells. *Annual Review of Immunology* **36,** 1–29 (2018).

63. Elliott, J. I. *et al.* Phosphatidylserine exposure in B lymphocytes: a role for lipid packing. *Blood* **108,** 1611–7 (2006).

64. Elliott, J. I. *et al.* Membrane phosphatidylserine distribution as a non-apoptotic signaling mechanism in lymphocytes. *Nature Cell Biology* **7,** 808–816 (2005).

65. Lentz, B. R. Exposure of platelet membrane phosphatidylserine regulates blood coagulation. *Progress in Lipid Research* **42,** 423–438 (2003).

66. Martin, S. *et al.* Immunologic stimulation of mast cells leads to the reversible exposure of phosphatidylserine in the absence of apoptosis. *Int Arch Allergy Imm* **123,** 249–258 (2000).

67. Bevers, E. M. & Williamson, P. L. Phospholipid scramblase: An update. *FEBS Letters* **584,** 2724–2730 (2010).

68. Nagata, S., Suzuki, J., Segawa, K. & Fujii, T. Exposure of phosphatidylserine on the cell surface. *Cell Death Differ* **23,** 952–961 (2016).

69. Segawa, K. *et al.* Caspase-mediated cleavage of phospholipid flippase for apoptotic phosphatidylserine exposure. *Science* **344,** 1164–1168 (2014).

70. Suzuki, J., Denning, D. P., Imanishi, E., Horvitz, R. H. & Nagata, S. Xk-Related Protein 8 and CED-8 Promote Phosphatidylserine Exposure in Apoptotic Cells. *Science* **341,** 403–406 (2013).

71. Fujii, T., Sakata, A., Nishimura, S., Eto, K. & Nagata, S. TMEM16F is required for phosphatidylserine exposure and microparticle release in activated mouse

platelets. *Proceedings of the National Academy of Sciences* **112,** 12800–12805 (2015).

72. Segawa, K., Suzuki, J. & Nagata, S. Constitutive exposure of phosphatidylserine on viable cells. *Proceedings of the National Academy of Sciences* **108,** 19246–19251 (2011).

73. Segawa, K. & Nagata, S. An Apoptotic 'Eat Me' Signal: Phosphatidylserine Exposure. *Trends in Cell Biology* **25,** 639–650 (2015).

74. Toda, S., Nishi, C., Yanagihashi, Y., Segawa, K. & Nagata, S. Current Topics in Developmental Biology. *Curr Top Dev Biol* **114,** 267–295 (2015).

75. van der Meer, J. H., van der Poll, T. & van Veer, C. TAM receptors, Gas6, and protein S: roles in inflammation and hemostasis. *Blood* **123,** 2460–2469 (2014).

76. Krahling, S., Callahan, M. K., Williamson, P. & Schlegel, R. A. Exposure of phosphatidylserine is a general feature in the phagocytosis of apoptotic lymphocytes by macrophages. *Cell Death Differ* **6,** 4400473 (1999).

77. Asano, K. *et al.* Masking of phosphatidylserine inhibits apoptotic cell engulfment and induces autoantibody production in mice. *J Exp Medicine* **200,** 459–467 (2004).

78. Hanayama, R. *et al.* Identification of a factor that links apoptotic cells to phagocytes. *Nature* **417,** 182–7 (2002).

79. Toda, S., Hanayama, R. & Nagata, S. Two-Step Engulfment of Apoptotic Cells. *Molecular and Cellular Biology* **32,** 118–125 (2012).

80. Yanagihashi, Y., Segawa, K., Maeda, R., Nabeshima, Y. & Nagata, S. Mouse macrophages show different requirements for phosphatidylserine receptor Tim4 in efferocytosis. *Proceedings of the National Academy of Sciences* **114,** 8800–8805 (2017).

81. Dransfield, I., Zagórska, A., Lew, E., Michail, K. & Lemke, G. Mer receptor tyrosine kinase mediates both tethering and phagocytosis of apoptotic cells. *Cell*

Death & Disease **6,** e1646 (2015).

82. Nakahashi-Oda, C. *et al.* Apoptotic epithelial cells control the abundance of Treg cells at barrier surfaces. *Nature Immunology* (2016). doi:10.1038/ni.3345

83. Savill, J., Dransfield, I., Gregory, C. & Haslett, C. A blast from the past: clearance of apoptotic cells regulates immune responses. *Nature Reviews Immunology* **2,** nri957 (2002).

84. Flannagan, R. S., Canton, J., Furuya, W., Glogauer, M. & Grinstein, S. The phosphatidylserine receptor TIM4 utilizes integrins as coreceptors to effect phagocytosis. *Molecular Biology of the Cell* **25,** 1511–1522 (2014).

85. Park, S.-Y., Bae, D.-J., Kim, M.-J., Piao, M. & Kim, I.-S. Extracellular Low pH Modulates Phosphatidylserine-dependent Phagocytosis in Macrophages by Increasing Stabilin-1 Expression. *J Biol Chem* **287,** 11261–11271 (2012).

86. Schroit, A. & Fidler, I. Effects of liposome structure and lipid composition on the activation of the tumoricidal properties of macrophages by liposomes containing muramyl dipeptide. *Cancer Res* **42,** 161–7 (1982).

87. Segawa, K. *et al.* Phospholipid flippases enable precursor B cells to flee engulfment by macrophages. *Proc National Acad Sci* **115,** 201814323 (2018).

88. Krishnaswamy, S. Prothrombinase complex assembly. Contributions of protein-protein and protein-membrane interactions toward complex formation. *The Journal of biological chemistry* **265,** 3708–18 (1990).

89. Jones, M. E., Lentz, B. R., Dombrose, F. A. & Sandberg, H. Comparison of the abilities of synthetic and platelet-derived membranes to enhance thrombin formation. *Thrombosis Research* **39,** 711–724 (1985).

90. Dillon, S. R., Constantinescu, A. & Schlissel, M. S. Annexin V Binds to Positively Selected B Cells. *J Immunol* **166,** 58–71 (2001).

91. Dillon, S. R., Mancini, M., Rosen, A. & Schlissel, M. S. Annexin V Binds to

Viable B Cells and Colocalizes with a Marker of Lipid Rafts upon B Cell Receptor Activation. *J Immunol* **164,** 1322–1332 (2000).

92. Demo, S. *et al.* Quantitative measurement of mast cell degranulation using a novel flow cytometric annexin-V binding assay. *Cytometry* **36,** 340–8 (1999).

93. Smrž, D., Dráberová, L. & Dráber, P. Non-apoptotic Phosphatidylserine Externalization Induced by Engagement of Glycosylphosphatidylinositol-anchored Proteins. *J Biol Chem* **282,** 10487–10497 (2007).

94. Rysavy, N. M. *et al.* Beyond apoptosis: the mechanism and function of phosphatidylserine asymmetry in the membrane of activating mast cells. *Bioarchitecture* **4,** 127–37 (2014).

95. Nakahashi-Oda, C., Tahara-Hanaoka, S., Honda, S., Shibuya, K. & Shibuya, A. Identification of phosphatidylserine as a ligand for the CD300a immunoreceptor. *Biochemical and Biophysical Research Communications* **417,** 646–650 (2012).

96. Poon, I. K., Lucas, C. D., Rossi, A. G. & Ravichandran, K. S. Apoptotic cell clearance: basic biology and therapeutic potential. *Nature Reviews Immunology* **14,** 166–180 (2014).

97. Okoshi, Y. *et al.* Requirement of the tyrosines at residues 258 and 270 of MAIR-I in inhibitory effect on degranulation from basophilic leukemia RBL-2H3. *International immunology* **17,** 65–72 (2004).

98. Lee, H. *et al.* Activation of human synovial mast cells from rheumatoid arthritis or osteoarthritis patients in response to aggregated IgG through Fcγ receptor I and Fcγ receptor II. *Arthritis and rheumatism* **65,** 109–19 (2013).

99. Harvima, I. T. *et al.* Molecular targets on mast cells and basophils for novel therapies. *The Journal of allergy and clinical immunology* **134,** 530–44 (2014).

100. Gelles, J. D. & Chipuk, J. Robust high-throughput kinetic analysis of apoptosis with real-time high-content live-cell imaging. *Cell Death Dis* **7,** e2493 (2016).

101. Leventis, P. A. & Grinstein, S. The distribution and function of phosphatidylserine in cellular membranes. *Annu Rev Biophys* **39,** 407–427 (2010).

102. Okoshi, Y. *et al.* Requirement of the tyrosines at residues 258 and 270 of MAIR-I in inhibitory effect on degranulation from basophilic leukemia RBL-2H3. *International immunology* **17,** 65–72 (2005).

103. Matsukawa, T. *et al.* Ceramide-CD300f binding suppresses experimental colitis by inhibiting ATP-mediated mast cell activation. *Gut* **65,** gutjnl-2014-308900 (2015).

104. Lalevée, S., Ferry, C. & Rochette-Egly, C. Transcription Factors, Methods and Protocols. *Methods Mol Biology Clifton N J* **647,** 251–266 (2010).

9. Acknowledgement

This dissertation work is performed in the Department of immunology in University of Tsukuba, where fantastic scientists gather and push the boundary of science. This dissertation will not be possible without the generous help from them.

I would like to express my deepest gratitude to my mentors Dr. Akira Shibuya and Dr. Nakahashi-Oda Chigusa. Their dedication to CD300a biology is the most critical determinant for the outcome of this project. Their passion of science, persistence on critical thinking, sense of novelty, precision of judgement and more constitute the most important mentorship I have ever experienced and benefited from. I am very grateful to this four-and-half-year training under their guidance and I believe their imprinting on me will continue benefit to my future career.

This PhD will not be possible without the continuous support from the lab community with sharing reagents, protocols, ideas and so on. Actually, it was during a casual chatting after dinner in the lab, the key idea of this project bubbled out. Specifically, I would like to thank Dr. Fujiyama Satoshi, Dr. Kazumasa Kanemaru, Dr. Tsukasa Nabekura, Mr. Yuuta Nakazawa and Ms. Mariana Silva Almeida for their generous help at any time upon my request, both mentally and scientifically.

Last but not least, I want to thank my beloved families, dad and mum, and my girlfriend, Wenjun. Without them, I could not have survived the difficult periods during this PhD. Their encouraging and caring always keep me moving forward.

10. Abbreviation

ATP	Adenosine triphosphate
ATP11C	ATPase Phospholipid Transporting 11C
BMMC	Bone marrow dirived mast cell
FceRI	High-affinity IgE receptor I
FRET	Fluorescence resonance energy transfer
IgE	Immunoglobulin E
ITAM	Immunoreceptor tyrosine-based activation motif
ITIM	Immunoreceptor tyrosine-based inhibition motif
MC	Mast cell
MHC	Major histocompatibility complex
NBD-PS	1,2-dioleoyl-sn-glycero-3-phospho-L-serine-N-(7-nitro-2-1,3-benzoxadiazol-4-yl
PA	Phosphatidic acid
PC	phosphatidylcholine
PE	Phosphatidylethanolamine
PI	Phosphatidylinositol
PS	Phosphatidylserine
PSA	Passive systemic anaphylaxis
SHIP	Src homology region 2 containing inositol phosphatase
SHP	Src homology region 2 domain-containing phosphatase-1
TNF	Tumor necrosis factor